Journal of South American Earth Sciences 125 (2023) 104286

Contents lists available at ScienceDirect

Journal of South American Earth Sciences

journal homepage: www.elsevier.com/locate/jsames

Sediment dispersal and basin evolution during contrasting tectonic regimes along the western Gondwanan margin in the central Andes

Amanda Z. Calle [a,b,c,*], Brian K. Horton [a,b], Raúl García [d], Ryan B. Anderson [e], Daniel F. Stockli [a], Peter P. Flaig [c], Sean P. Long [f]

[a] Department of Geological Sciences, Jackson School of Geosciences, University of Texas at Austin, Austin, TX, 78712, USA
[b] Institute for Geophysics, Jackson School of Geosciences, University of Texas at Austin, Austin, TX, 78712, USA
[c] Bureau of Economic Geology, Jackson School of Geosciences, University of Texas at Austin, Austin, TX, 78758, USA
[d] Instituto de Investigaciones Geológicas y Medio Ambiente (IGEMA), Universidad Mayor de San Andrés, La Paz, Bolivia
[e] Department of Geosciences, Idaho State University, ID, 83209, USA
[f] School of the Environment, Washington State University, WA, 99164, USA

ARTICLE INFO

Keywords:
Detrital zircon provenance
Pre-Andean basin evolution
Western Gondwana
Paleogeography of southern Bolivia
Famatinian magmatic arc
Transpampean Arch

ABSTRACT

A >15-20 km-thick succession in southern Bolivia forms the most-complete stratigraphic record in western Gondwana. Upper Neoproterozoic–Carboniferous clastic rocks record ~300 Myr of marine, nonmarine, and glacially influenced sedimentation in diverse basin systems generated by variable tectonic regimes along the western edge of Gondwana during active and passive-margin conditions. New provenance results help resolve key uncertainties regarding source regions and sediment dispersal patterns. The findings are integrated with spatial variations in stratigraphic thicknesses to evaluate regional patterns of basin subsidence, magmatism, and deformation during long-term evolution of the western Gondwanan margin in the central Andes.

Detrital zircon U–Pb geochronological data for 17 sandstone samples reveal sedimentary input from Precambrian cratonic basement provinces and pre-Andean basement, magmatic arc, and fold-thrust belt source regions. The basement age signatures indicate derivation from the flanking Brasiliano (900-560 Ma) and Pampean (650-500 Ma) provinces to the south and east, and the distal Rio de la Plata craton (2400-2000 Ma) along the eastern South American margin ~1000–1500 km to the southeast. Although the greater Amazonian craton was not a major contributor, subordinate Amazonian signatures from the Sunsás (1300-950 Ma) province to the east and northeast selectively fed the northern basin regions of the central Andes. Despite the lack of Paleozoic igneous rocks in Bolivia, detrital zircons of Ordovician age attest to the pre-Andean influence of the subduction-related Famatinian magmatic arc. Limited Devonian-Carboniferous igneous material was contributed locally from western pre-Andean highlands or regionally by axial northward transport from selected igneous sources in Argentina and Chile. Episodic recycling of Neoproterozoic–Paleozoic basin fill, including a sharp reappearance of Famatinian-age detritus, can be linked to periods of Paleozoic crustal shortening and foreland sedimentation ascribed to Famatinian, Ocloyic, Chañic, or Gondwanide phases of deformation.

The spatial distribution of sediment sources along with temporal shifts in sediment routing highlight several stages in the paleogeographic evolution of the western Gondwanan margin preserved in the central Andes. Initial regional subsidence spanned a multiphase Neoproterozoic to early Paleozoic history of Rodinia breakup, Brasiliano-Pampean orogenesis, and post-orogenic back-arc extension prior to final late Paleozoic amalgamation of Gondwana. The early Paleozoic onset of subduction and Famatinian arc magmatism led to high-magnitude subsidence (>10–15 km) likely driven by Ordovician slab rollback in an extensional back-arc basin. Thereafter, intermittent Paleozoic contraction in a poorly understood pre-Andean system (best expressed in the Eastern Cordillera of Bolivia and neighboring segments of northern Argentina and southern Peru) generated transient topographic loads that produced superimposed flexural foreland and successor basin systems.

* Corresponding author. Bureau of Economic Geology, Jackson School of Geosciences, University of Texas at Austin, Austin, TX 78758, USA.
E-mail address: amanda.calle@beg.utexas.edu (A.Z. Calle).

https://doi.org/10.1016/j.jsames.2023.104286
Received 16 December 2022; Received in revised form 28 February 2023; Accepted 28 February 2023
Available online 2 March 2023

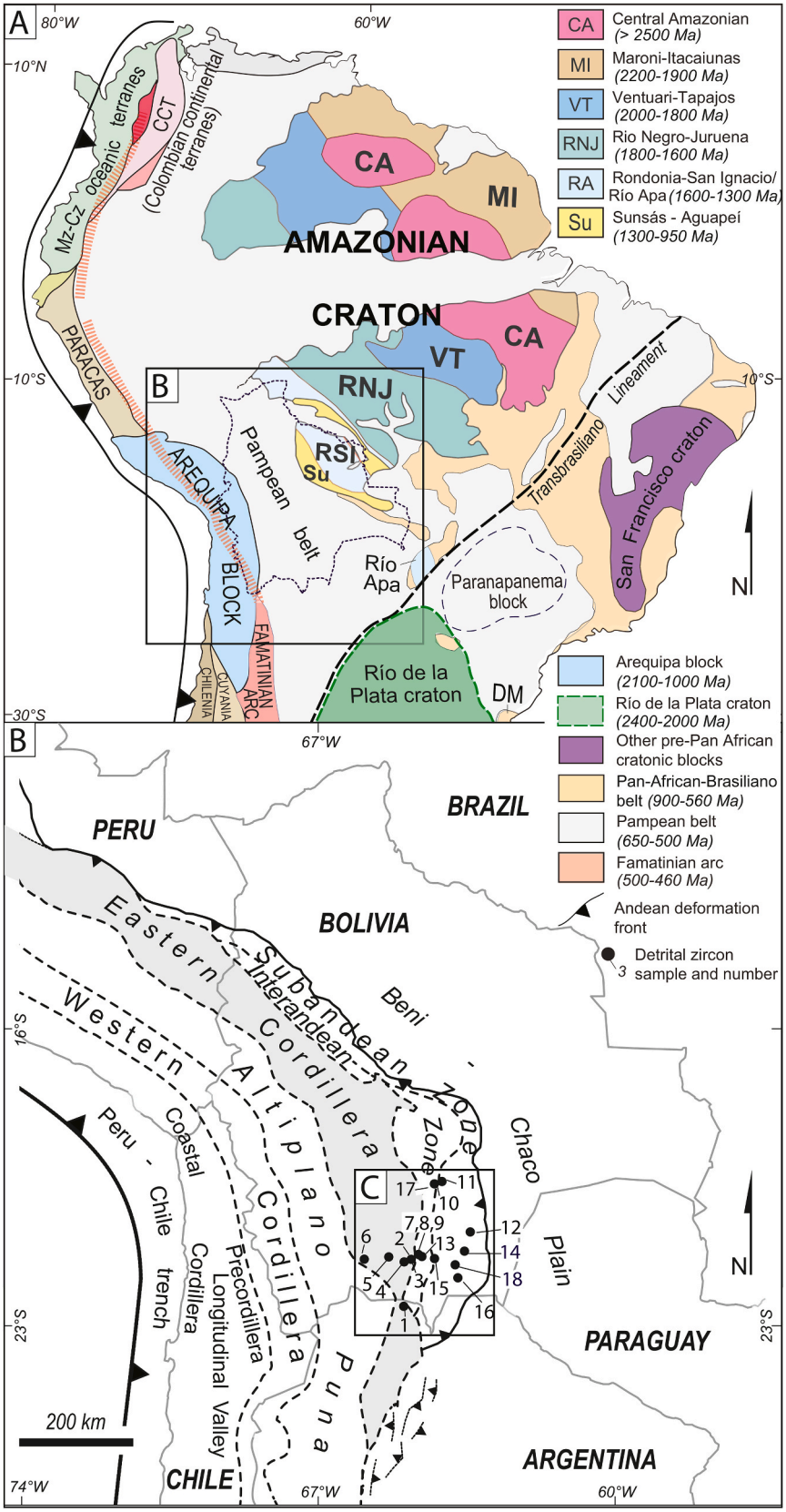

Fig. 1. (A) Map of the major tectonic provinces of South America, which are distinguished by the principal metamorphic/igneous ages (listed in the key). (B) Map of the study region in west-central South America showing sample locations in southern Bolivia relative to modern Andean tectonic provinces. Adapted from Loewy et al. (2004), Rapela et al. (2007), Favetto et al. (2015), Ramos (2010a), Ibanez-Mejia et al. (2015), Chew et al. (2016); Cordani et al. (2010b). (C) Southern Bolivia geological map (after Choque and Almendras, 2012) with detrital zircon sample locations.

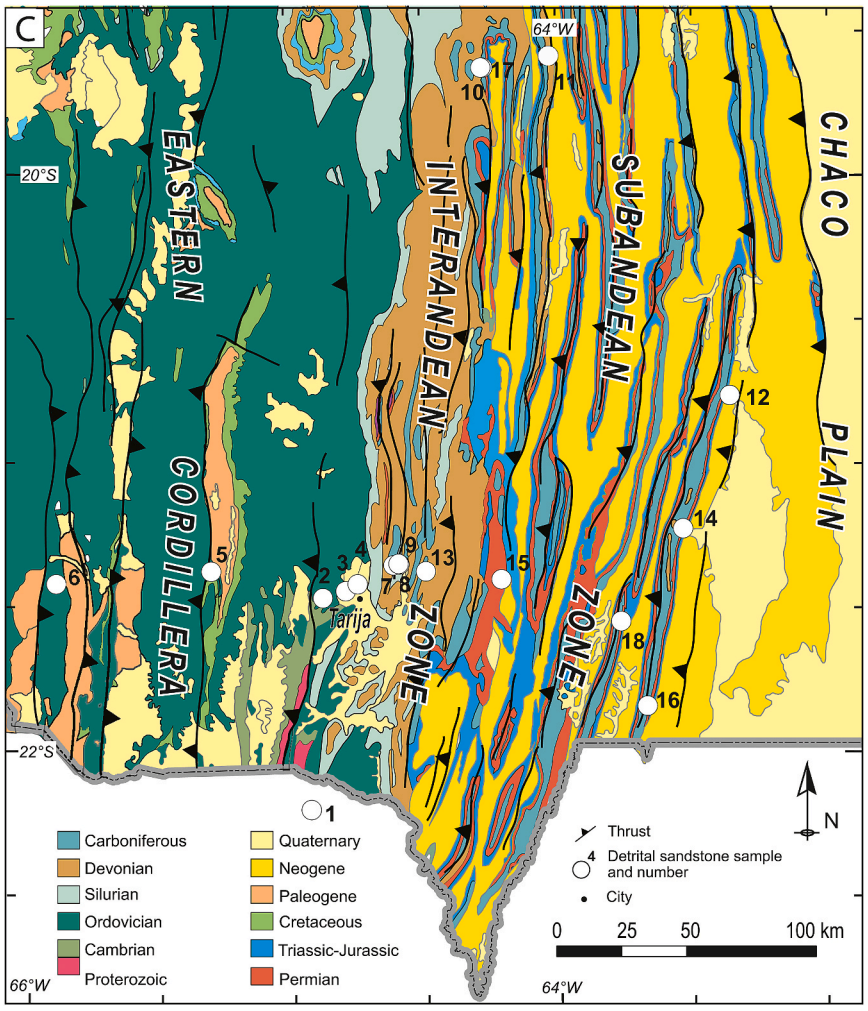

Fig. 1. (*continued*).

1. Introduction

Contrasting tectonic, magmatic, and sedimentary processes helped shape the pre-Andean paleogeography of the western Gondwanan margin and later growth of the Andean orogenic belt. Several major geologic transitions are expressed within the central segment of South America at ~10–25°S latitude (Fig. 1). Within the continental interior, the Precambrian Amazonian craton contrasts with separate basement provinces of variable age in southern South America (Cordani et al., 2003; Cordani and Teixeira, 2007; Rapela et al., 2007; Casquet et al., 2018). Along the western margin, the central Andes are distinguished by the presence of the Arequipa basement terrane (Coira et al., 1982; Loewy et al., 2004; Ramos, 2008). In Bolivia, the central Andes also lack strong records of Paleozoic tectonomagmatic events such as the Famatinian and Gondwanide orogenic episodes that profoundly affected other Andean regions (Ramos, 1988, 2009, 2018; Vujovich et al., 2004; Cawood, 2005; Rapela et al., 2016). These dissimilarities influenced not only the Neoproterozoic-Paleozoic evolution of western Gondwana but also the subsequent construction of the Andean orogenic belt and adjacent foreland, where major along-strike variations are observed in structural and stratigraphic records (Kley et al., 1999; McGroder et al., 2015; Horton, 2018a, 2018b).

The >15-20 km-thick succession of Bolivia provides a long-lived record of erosional exhumation and sediment dispersal from major cratonic and pre-Andean orogenic provinces during Neoproterozoic-Paleozoic evolution of diverse basin systems (Isaacson and Díaz-Martínez, 1995; Sempere, 1995; Starck, 1995; Jaillard et al., 2000; Suárez-Soruco, 2000). Several key issues remain unresolved. (1) Whereas Precambrian rocks in the South American interior are considered the most likely sources of sediment, there are no estimates of the relative contributions of northern (Amazonian) versus southern basement provinces. (2) Further uncertain is the influence of pre-Andean subduction-related magmatism and deformation (including the Famatinian, Ocloyic, Chañic, and Gondwanide orogenic episodes) on Paleozoic sediment dispersal and basin filling. (3) The importance of glaciation and erosional recycling of Paleozoic basin fill remains unclear. (4) Finally, despite the exceptional stratigraphic thickness, the regional geometries and mechanisms of basin subsidence have not been fully explored.

In this paper, we present detrital zircon U–Pb geochronological results for 17 Paleozoic sandstones (~1700 analyses) from southern Bolivia and integrate these data with published U–Pb results for neighboring zones of the central Andes. This provenance information is combined with isopach data, paleocurrents, and regional chronostratigraphic constraints to reconstruct the paleogeography, sediment dispersal patterns, and basin accommodation mechanisms in the central Andes during evolution of the western Gondwanan margin. Our study further highlights uncertainties regarding subduction geometries, tectonic configurations, and the potential role of tectonic inheritance on later Andean orogenesis.

2. Geologic setting

The central Andes and adjacent foreland represent a spatial

transition between contrasting geologic elements of northern and southern South America (Figs. 1 and 2). The Amazonian craton of northern South America contains an Archean-Paleoproterozoic nucleus flanked to the west by successively younger basement provinces, including the Mesoproterozoic Sunsás (Grenville) and Neoproterozoic Brasiliano (Pan-African) belts (e.g., Litherland and Bloomfield, 1981; Cordani et al., 2003, 2010a, 2010b; Cordani and Teixeira, 2007; Basei et al., 2010). In contrast, southern South America contains varied basement terranes consisting of the Paleoproterozoic Río de la Plata craton along the eastern continental margin flanked to the west by the Mesoproterozoic-Neoproterozoic Pampean orogenic belt (Ramos, 1988; Litherland et al., 1989; Rapela et al., 2007; Casquet et al., 2018). The west-central (central Andean) segment of South America is underpinned by Paleoproterozoic-Mesoproterozoic basement rocks of the Arequipa terrane (Loewy et al., 2004; Ramos, 2008; Casquet et al., 2010).

The central Andes exhibit the thickest Phanerozoic sedimentary cover and maximum orogenic width (Horton et al., 2022). The pre-Andean history has been attributed to a complex combination of Neoproterozoic–Mesozoic passive and active-margin conditions with contrasting tectonic regimes (tensile, contractile, strike-slip, and neutral stress conditions) and pronounced phases of Paleozoic glaciation (Fig. 2; Franz et al., 2006; Reimann et al., 2010; Anderson, 2011). Later growth of the central Andes was accommodated by principally Cenozoic retro-arc shortening, with associated orogenic exhumation and foreland basin sedimentation.

At ~21°S, the central Andes consist of several north-trending tectonomorphic zones and basin systems (Fig. 1C). In the west, these zones include the Peru-Chile trench, Coastal Cordillera (Mesozoic magmatic arc), Longitudinal Valley (modern forearc, overprinting a late Paleozoic arc), Precordillera (Paleogene arc), Western Cordillera (Neogene arc), and the Altiplano-Puna plateau (Neogene hinterland basin). In the east, the Eastern Cordillera defines a bivergent thrust belt that exhumes Ordovician rocks overlain unconformably by Jurassic-Neogene strata (Kley et al., 1997; DeCelles and Horton, 2003; McQuarrie et al., 2005). To the east, the Interandean Zone and Subandean Zone define a thin-skinned fold-thrust belt composed of Silurian–Cretaceous rocks blanketed by Cenozoic fill of the Chaco foreland basin (Kley, 1996; Uba et al., 2009; Calle et al., 2018).

3. Neoproterozoic–Paleozoic stratigraphic framework

The >15-20 km-thick Neoproterozoic–Paleozoic stratigraphic succession of southern Bolivia (Fig. 3) recorded principally marine sedimentation along the western margin of Gondwana. Neoproterozoic to mid-Cambrian accumulation of >3 km of deep-water turbidites to shallow-marine clastic and limited carbonate deposits produced the Puncoviscana Formation (Jêzek et al., 1985; Litherland et al., 1989; Omarini et al., 1999; Aceñolaza and Toselli, 2009; Escayola et al., 2011).

A >12 km thick upper Cambrian–Ordovician section (Fig. 3) of fluvial, deltaic, and deep-marine deposits documented a rapidly subsiding basin (Suárez-Soruco, 1976, 2000; Sanchez and Salfity, 1999; Aceñolaza, 2003; Egenhoff, 2007; Augustsson et al., 2011). Westward progradation of the continental margin (~2 km thick Sama and Iscayachi Formations) was followed by Ordovician igneous activity in the Famatinian magmatic arc and mud-rich deep-sea fan deposition (~10 km thick Cieneguillas, Agua y Toro, Marquina, and additional Formations) in a back-arc setting. Sparse Ordovician volcaniclastic deposits in western Bolivia (Tistl, 1985; Avila-Salinas, 1992, 1996)

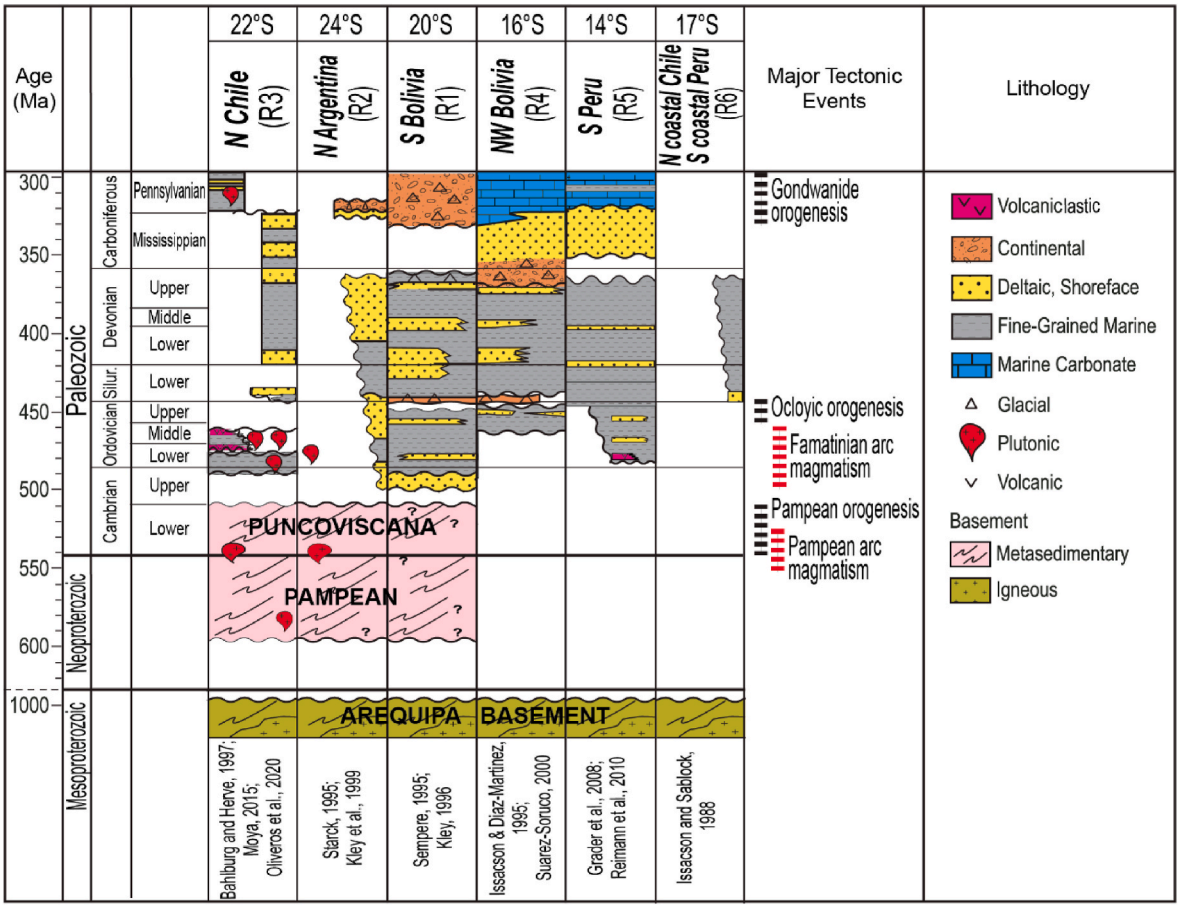

Fig. 2. Chart displaying comparative ages, lithologies, and tectonic events recorded by basement units and cover strata within six representative regions (R1-R6) of west-central South America (after McGroder et al., 2015). Note the mostly continuous Neoproterozoic-Carboniferous succession in southern Bolivia (R1).

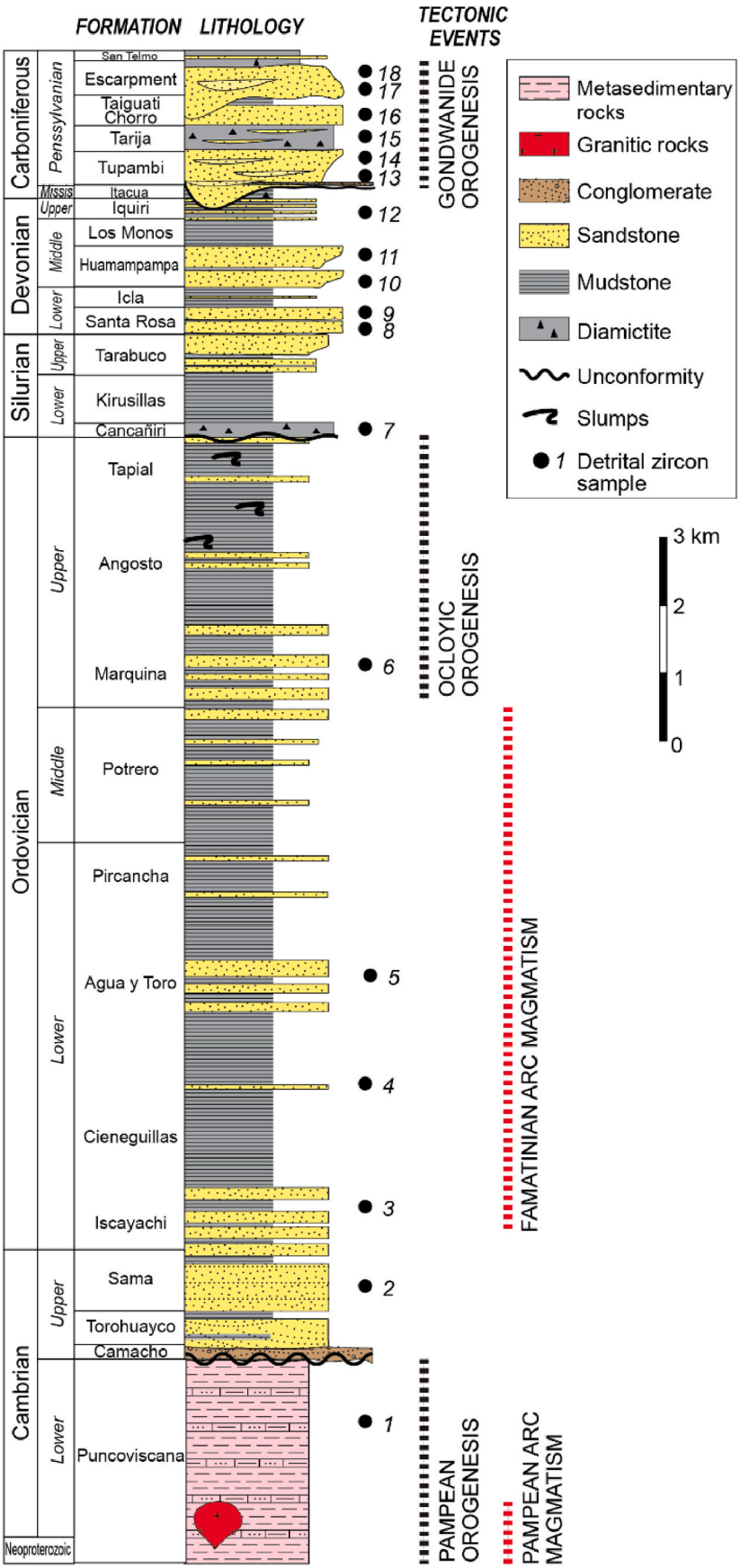

Fig. 3. Generalized Neoproterozoic-Paleozoic stratigraphic column for southern Bolivia depicting lithologies, unconformities, and 18 sample locations (sample 1 is from Escayola et al., 2011). Neoproterozoic-Cambrian metasedimentary basement is capped by a ~15 km thick Paleozoic succession of principally clastic deposits representative of marine and nonmarine conditions.

correlate with Famatinian volcanic and marine clastic strata of northern Argentina and Chile (Castaños and Rodrigo, 1978; Coira et al., 1982, 2009; Ramos, 1988; Bierlein et al., 2006). Late Ordovician basin closure was associated with fold-thrust deformation and low-grade metamorphism during the 460–440 Ma Ocloyic orogeny (Fig. 3; Mon and Salfity, 1995; Bahlburg and Hervé, 1997; Egenhoff, 2007; Moya, 2015), which may be considered the final phase of the broadly defined Cambrian-Ordovician Famatinian orogeny (Ramos, 2018; Otamendi et al., 2020).

Upper Ordovician–Lower Silurian deposits (>1.4 km Cancañiri Formation) recorded an apparent deepening of the marine back-arc basin (Suárez-Soruco, 2000; Gagnier et al., 1996; Schönian and Egenhoff, 2007). The overlying Silurian–Devonian sand-rich marine units (>3.5 km thick Tarabuco-Santa Rosa, Huamampampa and Iquiri Formations) recorded progradation to the ENE away from an orogenic highland with little or no arc magmatism (Fig. 3; Gohrbandt, 1992; Isaacson and Díaz-Martínez, 1995; Arispe and Díaz-Martínez, 1996; Limachi et al., 1996; Miranda et al., 2003).

A sea-level fall and regional glaciation induced deep dissection of Upper Devonian rocks and subsequent Carboniferous deposition of glacially influenced fluvial, deltaic, lacustrine and shallow marine deposits (>2 km Machareti and Mandiyuti groups) (Fig. 3; Starck, 1995; di Pasquo, 2007; Grader et al., 2008; Wicander et al., 2011; Anderson, 2011; Bache et al., 2012). The absence of Devonian-Carboniferous strata across much of the Altiplano-Puna plateau and Eastern Cordillera of western Bolivia and northernmost Argentina may be attributable to regional shortening and uplift of a mid-Paleozoic structural high, the Transpampean Arch (Tankard et al., 1995; McGroder et al., 2015).

Collectively, the clastic sediments that dominate the Neoproterozoic-Carboniferous succession in the central Andes may derive from a range of source regions, including Precambrian cratonic provinces, additional Precambrian basement rocks in the Andes and adjacent foreland, Neoproterozoic metasedimentary cover rocks, and igneous and recycled sedimentary materials in pre-Andean magmatic arc and fold-thrust belt source regions.

4. Potential sediment source regions

To identify and track sediment sources through time, we summarize the cratonic provinces, basement terranes, and sedimentary assemblages that may have supplied sediment to Neoproterozoic-Paleozoic basins along the western Gondwanan margin (Fig. 1).

4.1. Amazonian craton (2500–950 Ma)

To the east and northeast of the central Andean study area, the Amazonian craton (Fig. 1A) consists of an Archean-Paleoproterozoic nucleus (>2000 Ma) flanked to the west by successively younger basement provinces, including the Ventuari-Tapajos (2000–1800 Ma), Rio Negro-Juruena (1800–1600 Ma), Rondonia-San Ignacio (1600–1300 Ma), and Sunsás-Aguapei (1300–950 Ma) provinces (Litherland et al., 1989; Geraldes et al., 2001; Bettencourt et al., 2010; Teixeira et al., 2010). Isolated exposures of the Río Apa craton are considered the southernmost continuation of the Amazonian craton (Cordani et al., 2010b; Faleiros et al., 2016). The Sunsás province, consisting of granitic intrusions, mafic sills, and metasedimentary rocks, lies in closest proximity to the Andes and is partially buried by Cenozoic foreland basin fill. Widespread 1300–950 Ma detrital zircons in the northern and central Andes suggest that Sunsás basement forms a continuous ~5000 km long belt in the present Andean foreland from ~10°N to ~25°S (e.g., Chew et al., 2007; Santos et al., 2008; Ramos, 2010a; Teixeira et al., 2010; Ibanez-Mejia et al., 2015).

4.2. Brasiliano belt (~900–560 Ma)

East of the study region, widely distributed 900–560 Ma granitic and volcanic rocks of the Neoproterozoic Brasiliano belt weld the Amazonian craton to the San Francisco, Río de la Plata and other cratonic rocks of South America (Fig. 1A) (Litherland et al., 1989; Geraldes et al., 2001, 2015; Cordani et al., 2003). Along the eastern continental margin, the Dom Feliciano belt contains granitic and metasedimentary rocks formed during Brasiliano orogenesis (Oriolo et al., 2016; Hueck et al., 2018). The Brasiliano belt also encompasses the NE-trending Transbrasiliano lineament and is partially correlative with associated sedimentary rocks of the Paraguay belt, a fold-thrust system contemporaneous with Pampean orogenesis during the late Neoproterozoic (Litherland and Bloomfield, 1981; Campanha et al., 2010; Cordani et al., 2010a; Walde et al., 2015; D'el-Rey Silva et al., 2016).

4.3. Río de la Plata craton (2400–2000 Ma)

To the southeast, the Río de la Plata craton forms the largest Precambrian crustal province in southern South America, with Paleoproterozoic igneous and metamorphic rocks formed at 2400–2000 Ma (Fig. 1A). In the Andean foreland of Argentina, the NNE-trending structural boundaries of the Río de la Plata craton are overlapped by Neoproterozoic-lower Cambrian metasedimentary rocks of the Puncoviscana Formation (Rapela et al., 2007; Favetto et al., 2015; Girelli et al., 2018).

4.4. Pampean orogen and Puncoviscana basin (~650–500 Ma)

The mostly buried Pampean orogenic belt (or Pampia terrane) beneath the central Andean foreland is situated between the Sunsás province (westernmost Amazonian craton) and the Arequipa basement of the westernmost central Andes (Fig. 1A). The Pampean orogen is dominated by 555–500 Ma igneous and metamorphic ages superimposed on precursor Precambrian basement with Nd model ages (TDM) of ~1800, 1600–1300, and/or 1300–950 Ma (Litherland et al., 1989; Franz et al., 2006; Schwartz et al., 2008; Ramos et al., 2010; Pepper et al., 2016). Pampean basement is overlain by clastic low-grade metasedimentary rocks of the Neoproterozoic–lower Cambrian Puncoviscana Formation (Jêzek et al., 1985; Becchio et al., 1999; Aceñolaza et al., 2002; Suárez-Soruco, 2000). Published detrital zircon ages for the Puncoviscana basin suggest 1300-950 Ma and 700-530 Ma grains derived from Sunsás and Pampean-Brasiliano basement rocks (e.g., Adams et al., 2011; Escayola et al., 2011; Einhorn et al., 2015).

4.5. Arequipa block (2100–1000 Ma)

West of the study region, the Arequipa-Antofalla terrane forms Paleoproterozoic (2100–1800 Ma) and Mesoproterozoic (1300–1000 Ma) granitic basement of the forearc and western flank of the central Andes at 14–26°S (Fig. 1A) (Lehmann, 1978; Tosdal, 1996; Loewy et al., 2004; McLeod et al., 2013; Jiménez, 2018). This basement block was affected by a 1300–1000 Ma Sunsás-Grenville tectonothermal event and 700–400 Ma magmatism during Pampean and Famatinian orogenesis (Becchio et al., 1999; Lucassen et al., 2000; Wörner et al., 2000; Loewy et al., 2004; Franz et al., 2006; Casquet et al., 2010; Pankhurst et al., 2016; Rapela et al., 2016).

4.6. Famatinian magmatic arc (500–460 Ma) and Ocloyic orogeny (460–440 Ma)

In the central Andes, the north-trending Famatinian belt (Fig. 1A) represents a pre-Andean magmatic arc formed during Ordovician growth and retreat of an east-dipping subduction zone (e.g., Ramos, 2010a; Ducea et al., 2015; Otamendi et al., 2017; Rapela et al., 2018). Subduction-related igneous activity at 500-460 Ma was widespread in western Argentina, but the northern continuation of Famatinian magmatic arc is poorly resolved, with no major igneous sources documented in Bolivia. Famatinian magmatism was followed by 460–440 Ma

shortening and metamorphism associated with the Late Ordovician–Silurian Ocloyic orogeny, which involved consolidation of the offshore Famatinian arc and Arequipa block against west-central South America (Mon and Salfity, 1995; Bierlein et al., 2006).

4.7. Paleozoic basin fill

Paleozoic sedimentary rocks west of the study region are considered a potential source of recycled clastic material originally derived from the aforementioned basement and magmatic-arc sources. Evidence for such Pre-Andean recycling derives from several relationships within the central Andes. In western localities, Devonian–Carboniferous deposits are largely absent from the Altiplano of Bolivia, potentially due to nondeposition or erosion across a regional structural high that involved uplifted Arequipa basement (Isaacson and Díaz-Martínez, 1995). Similarly, a regional unconformity in which various Mesozoic units overlap Ordovician deep-water deposits across the Eastern Cordillera of Bolivia and northernmost Argentina documents the absence of Silurian–Carboniferous units that are preserved in adjacent regions (Kley, 1996; Kley et al., 1997; Anderson et al., 2017). The erosional removal of thick Paleozoic clastic deposits may have occurred during a single phase of exhumation, or incrementally during the successive Famatinian, Ocloyic, Chañic, and Gondwanide episodes of deformation.

5. Methods

Detrital zircon U–Pb geochronological results for 17 sandstone samples from Cambrian to Carboniferous units of southern Bolivia (19–22°S) clarify the depositional ages and sediment provenance within diverse basin settings developed along the long-lived pre-Andean margin (Figs. 1–3; Table S1, Supplementary data).

Detrital zircons were separated using standard methods of rock crushing, grinding, water table, heavy liquid, and magnetic separation. U–Pb analyses were conducted at the University of Texas at Austin using laser ablation inductively coupled plasma mass spectrometry (LA-ICP-MS) following procedures outlined by Levina et al. (2014) and Horton et al. (2016). For each sample, ~120 non-polished, tape mounted, randomly selected detrital zircon grains were analyzed using a PhotonMachine Analyte G.2 Excimer laser (30 μm laser spot size) with a large-volume Helex sample cell and a Thermo Element2 ICP-MS. Corrections for depth-dependent and elemental fractionation were accomplished by co-analysis of interspersed GJ1 as a primary zircon standard (600.4 ± 0.1 Ma; Jackson et al., 2004). In addition, Plesovice (337.2 ± 0. 4 Ma; Slama et al., 2008) was analyzed as a secondary standard to monitor procedural performance. U–Pb data were then reduced using the Iolite data reduction software VizualAge (Paton et al., 2010; Petrus and Kamber, 2012).

U–Pb ages and 2σ uncertainties are reported for analyses with <10% $^{206}Pb/^{238}U$ uncertainties, <20% discordance, and <5% reverse discordance (Table S1, Supplementary data). Reported ages represent $^{206}Pb/^{238}U$ ages for grains younger than 950 Ma and $^{207}Pb/^{206}Pb$ ages for older grains. Estimates of maximum depositional age (Fig. S1, Supplementary data) were derived from grains yielding <5% discordant $^{206}Pb/^{238}U$ and $^{207}Pb/^{235}U$ ages. Calculations of maximum depositional age (MDA) involved the weighted mean of the youngest concordant ages ($n \geq 3$) that overlapped within 2σ error (Dickinson and Gehrels, 2009), an unmixed routine to model the individual youngest significant peak ($n \leq 6$), and a TuffZirc age that identifies the youngest mode (Coutts et al., 2019). Systematically, the preferred MDA was in accordance with available bio-stratigraphic age constraints.

U–Pb results are displayed as probability density functions and age histograms, and are organized by stratigraphic level (Figs. 4–5). For diagnosing key provenance signatures, the plotted age spectra are presented into two columns, with 300–2000 Ma (right) and 300–800 Ma (left) age ranges, and >2000 Ma age populations shown (insets) where significant. For statistical comparison of U–Pb spectra, we employed a multidimensional scaling (MDS) plot (Fig. 6), which displays the D values from the Kolmogorov-Smirnov test (K–S test) (Saylor and Sundell, 2016). This two-dimensional plot identifies greater similarity for samples that spatially cluster together and less similarity for those that plot farther apart. To evaluate whether the MDS plot accurately represents dissimilarity between samples (goodness of fit), a Shepard plot is presented, with a stress factor = 0 for a perfect goodness of fit and >0.2 for a poor goodness of fit. After cross-correlating the geologic criteria, the MDS plot facilitates definition of three geographic source regions characterized by a fair goodness of fit (stress = 0.130) (Fig. 6).

6. Detrital zircon U–Pb geochronology

U–Pb results are presented for 18 samples from upper Neoproterozoic to Carboniferous strata (Figs. 3–6), including 17 new samples from southern Bolivia and a single published sample (Escayola et al., 2011) from northernmost Argentina. Cumulative U–Pb age distributions (Fig. 4) for all samples (N = 18, n = 1727 ages) depict the major components, classified according to age ranges that are representative of key source regions (Fig. 1).

The dominant cratonic and pre-Andean basement sources include (1) late Ediacaran to Cambrian (650–500 Ma) ages of the Pampean belt and (2) Tonian to mid-Ediacaran (900–560 Ma) ages from the Brasiliano province. The major pre-Andean igneous and metamorphic sources are represented by (1) Famatinian (500–460 Ma) and (2) Ocloyic (460–440 Ma) age components. Additional, less-common sources include the western Amazonian craton, as defined by (1) Mesoproterozoic (1300–950 Ma) ages from the Sunsás-Arequipa belt and Paleoproterozoic (2000–1350 Ma) ages from the Rondonia-San Ignacio or Río Apa province. A single sample records the exceptionally rare appearance of

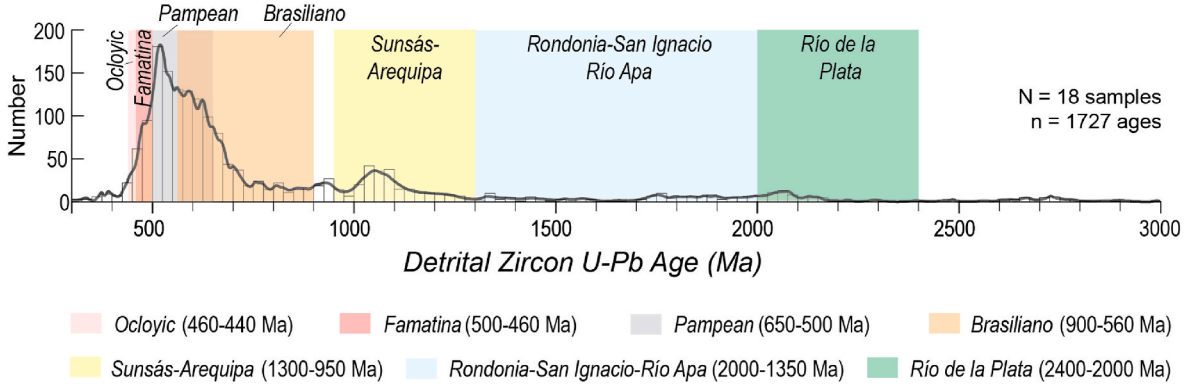

Fig. 4. Probability density plot with age histogram showing the composite U–Pb zircon age distribution for the 18 Paleozoic samples considered in this study. Color shading highlights the potential sediment source regions and associated tectonic episodes of west-central South America.

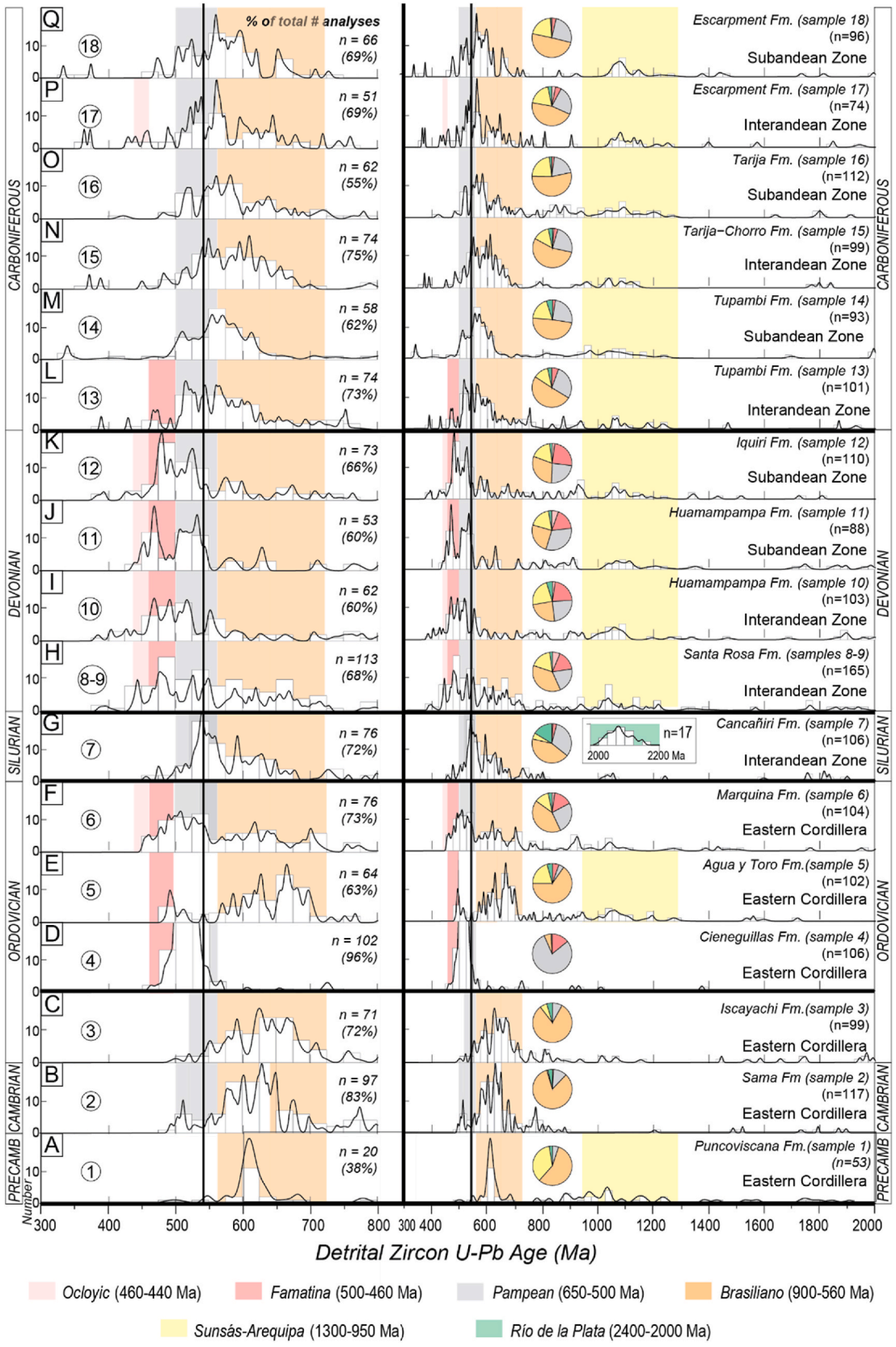

Fig. 5. Normalized probability density plots with age histograms (25 Myr bin size) and pie diagrams showing U–Pb age distributions for Neoproterozoic-Paleozoic samples from southern Bolivia. Color shading highlights the presence of particular age categories, in stratigraphic order (with Neoproterozoic-Cambrian basement rocks at the base and Carboniferous deposits at the top). Thicker black vertical line divides the datasets into two columns, with 300–2000 Ma (right) and 300–800 Ma (left) age ranges, and >2000 Ma age populations (insets) shown where significant. Horizontal black lines divide samples with similar provenance sources; vertical black lines separate Neoproterozoic and older, versus Cambrian and younger U–Pb ages.

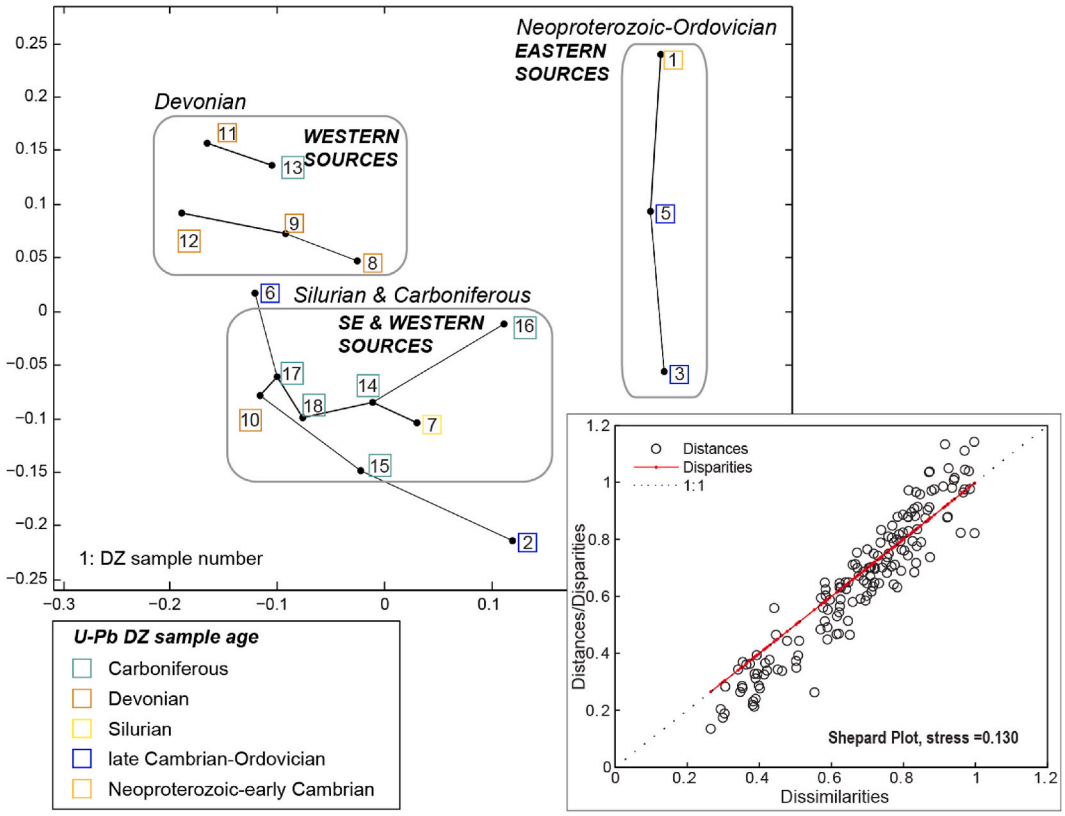

Fig. 6. Multidimensional scaling (MDS) and Shepard plots (stress = 0.130) based on detrital zircon U–Pb results for Neoproterozoic-Carboniferous samples from southern Bolivia, showing three discrete clusters of potential sediment sources (rectangular fields): Neoproterozoic-Ordovician samples indicative of eastern sediment sources, Devonian samples derived from western regions, and Silurian and Carboniferous samples from southeastern and probable western sources.

Archean age (2200–2000 Ma) detritus from the Río de la Plata craton.

The U–Pb results for the 18 samples (Fig. 5) are described in five separate age groups, according to similarities in U–Pb age distributions that reflect comparable sediment source regions (Fig. 6). The results also allow general assessments of maximum depositional age (MDA) for five samples (Fig. S1, Supplementary data), which reinforce past bio-stratigraphic age assignments.

6.1. Neoproterozoic–earliest Ordovician (samples 1–3)

In lowermost stratigraphic levels, upper Neoproterozoic–lowermost Ordovician strata (samples 1–3, Fig. 5A–C) shows signatures of cratonal sources to the east. Sample 1 (sample VLE07-109 of Escayola et al., 2011) from the upper Neoproterozoic–lower Cambrian Puncoviscana Formation contains dominantly 620–600 Ma Brasiliano ages, along with multicomponent 1300–950 Ma Sunsás and minor 2000–1350 Ma Rondonia-San Ignacio or Río Apa signatures (Fig. 5A). This age distribution reflects eastern sources including the Brasiliano province and western Amazonian craton, consistent with west-directed paleocurrents (Jèzek et al., 1985; Aceñolaza and Toselli, 2009).

Samples 2 and 3 (Fig. 5B and C) from the upper Cambrian Sama Formation and basal Ordovician Iscayachi Formation are defined by age peaks of 720–540 Ma and scattered 900–720 Ma and 560–520 Ma signatures derived almost exclusively from the Brasiliano province. A subordinate Pampean signature is defined by 550–520 Ma U–Pb zircon ages that complement an emergent 520–490 Ma peak indicative of Cambrian magmatism (MDA of 507.5 ± 2.6 Ma; Fig. S1A), in accordance with the middle-late Cambrian bio-stratigraphic age and stratigraphic position above the trilobite-bearing Lizoite and Campanario Formations (Aceñolaza, 2003; Egenhoff, 2007).

6.2. Ordovician (samples 4–6)

Within the thick Ordovician section, samples 4–6 (Fig. 5D–F) record the introduction of coeval magmatic arc signatures that complement multicomponent detrital signatures from established and new basement sources. The Lower Ordovician Cieneguillas Formation (sample 4, Fig. 5D) exhibits a restricted 550–480 Ma age distribution consistent with local input from Pampean basement (Augustsson et al., 2011; Aparicio-González et al., 2014) and the introduction of Early Ordovician ages from the newly established Famatinian arc.

The Lower Ordovician Agua y Toro Formation (sample 5, Fig. 5E) and Upper Ordovician Marquina Formation (sample 6; Fig. 5F) mark the return of eastern cratonic detritus, with broadly distributed age spectra that include Brasiliano (720–540 Ma) and Sunsás (1300–950 Ma) signatures. Sample 6, however, contains a greater proportion of pre-Andean source material, with 560–440 Ma ages corresponding to more-proximal Pampean, Famatinian, and Ocloyic signatures. The Cambrian-Ordovician age components are consistent with pre-Andean source regions involving contemporaneous arc magmatism, erosion of Pampean basement, and recycling of clastic fill from the Puncoviscana and other Cambrian-Ordovician basins (Egenhoff, 2007; Augustsson et al., 2015; Einhorn et al., 2015).

Three Ordovician samples (samples 4–6; Fig. 5D–F) include latest Cambrian-Early Ordovician ages from the coeval magmatic arc (Fig. S1), yielding MDA values of 483.2 ± 5.9 Ma (sample 4, Fig. S1B), 491.9 ± 3.1 Ma (sample 5, Fig. S1C), and 475.6 ± 4.1 Ma (sample 6, Fig. S1D). These ages are consistent with reported bio-stratigraphic ages for Bolivia (Suárez-Soruco, 2000; Erdtmann et al., 1995) and the correlative Santa Rosita Formation in Argentina (Basei et al., 2010; Toselli et al., 2012).

6.3. Silurian (sample 7)

The Lower Silurian Cancañiri Formation (sample 7, Fig. 5G) shows a distinctive age distribution indicative of proximal and distal sediment source regions. Late Neoproterozoic–Cambrian ages present in this Silurian sample are comparable to signatures in underlying units. However, in contrast to Ordovician samples, there are no syndepositional ages and no strong Famatinian-Ocloyic age peaks, suggesting no direct link to the extinct Famatian magmatic arc and associated metamorphic belt. The glacially influenced Cancañiri Formation (sample 7, Fig. 5G) is further distinguished by the singular appearance of 2200–2000 Ma detritus likely derived from the Río de la Plata craton, consistent with long-distance (>1500 km) transport potentially linked to large ice sheets (e.g., Starck et al., 2021).

6.4. Devonian (samples 8–12)

Fluvial to shallow-marine Devonian units (samples 8–12; Fig. 5H-L) show detrital zircon U–Pb age signatures attributable to proximal western sources of recycled sedimentary basin fill, older magmatic arc rocks, and pre-Andean basement. Relative to underlying formations, the five samples from the Devonian Santa Rosa, Huamampampa, and Iquiri Formations record an increase in widely distributed (or cosmopolitan) age components (Fig. 5). This includes the appearance and sustained presence of a dominant 500–440 Ma Famatinian-Ocloyic age signature, strong 560–500 Ma Pampean-Cambrian age peaks, and a broad range of subordinate 720–560 Ma Brasiliano ages. Devonian samples also show an increased proportion of the 1350–950 Ma Sunsás-Arequipa signature relative to underlying units.

The coeval occurrence of Ordovician and Mesoproterozoic ages points to sediment derivation from western sources that included the relict Famatinian arc and Arequipa basement. Additional proximal sources included basin fill and Pampean basement of late Neoproterozoic to Silurian age. The dominance of these pre-Andean sources over eastern cratonic sources is expressed in the discrete MDS clustering of Devonian samples relative to other samples (Fig. 6). A highly restricted set of roughly 410–370 Ma zircons suggest some degree of syndepositional Devonian magmatism, although the location and geologic context for such magmatism is unknown.

6.5. Carboniferous (samples 13–18)

Glacially influenced nonmarine and marine strata within the Carboniferous succession (samples 13–18, Fig. 5L–Q) yield similar detrital zircon age distributions indicative of a major provenance switch from western pre-Andean sources to chiefly Precambrian sources to the south and east. Six samples from the Pennsylvanian Tupambi, Tarija, Chorro, and Escarpment Formations (samples 13–18; Figs. 5 and 6) consistently show major 640–560 Ma Brasiliano age peaks and subordinate 560–520 Ma Pampean, 1300–950 Ma Sunsás-Arequipa, and 360–300 Ma Carboniferous ages.

A distinct shift from dominantly Paleozoic to dominantly Precambrian age peaks is manifest in the nearly complete elimination of Famatinian-Ocloyic ages and the reintroduction of major Brasiliano age components consistent with Pampean and Puncoviscana sources to the south and east. MDS comparisons of the internally consistent detrital zircon populations of Carboniferous samples with underlying samples demonstrate a sharp distinction from Devonian units and a shared provenance with the Silurian Cancañiri Formation (Figs. 5 and 6). This is consistent with a pronounced reduction in western sources (such as the relict Famatinian magmatic arc) and the enhanced influence of cratonal sources to the southeast that were previous contributors during Silurian basin evolution. A distal glacial provenance from the south/southeast is supported by the regional orientation of glacially carved paleovalleys of Carboniferous age (Starck, 1995; Tankard et al., 1995).

Although limited, Famatinian-Ocloyic and Carboniferous age zircons (Fig. 5) suggest modest recycling of older basin fill and/or minor input from western pre-Andean highlands. A single sample from the Tupambi Formation yields a MDA of 340.2 ± 5.3 Ma (sample 14, Fig. S1E), slightly older than palynological age estimates (e.g., Rocha-Campos et al., 1977; di Pasquo, 2007; Wicander et al., 2011), indicative of renewed syndepositional arc magmatism along the western continental margin.

7. Sediment dispersal patterns and paleogeographic reconstructions

The integration of new and published detrital zircon U–Pb results (Fig. 7; Tables S1 and S2) provides the foundation for generalized map-view reconstructions of sediment provenance patterns and paleogeography along the pre-Andean margin (Fig. 8). The geochronological results derive from six central Andean regions (R1-R6) between 9° and 26°S: southern Bolivia (R1, this study); northern Argentina (R2); northern Chile (R3); northwestern Andean Bolivia (R4); southern Peru (R5); and northernmost coastal Chile to southernmost coastal Peru, R6). Our emphasis in employing this expanded U–Pb database is to utilize Neoproterozoic to Carboniferous stratigraphic variations in key detrital signatures (Figs. 5–6) to discriminate sediment source regions through time (Fig. 8).

To evaluate changes in basin geometry, the expanded provenance results are assessed in coordination with isopach maps that show the regional distribution of stratigraphic thicknesses. Although not available for all time slices, previously published Silurian, Devonian, and Carboniferous isopach maps were key for this evaluation (Isaacson and Sablock, 1988; Gohrbandt, 1992; Reutter et al., 1994; Wiens, 1995; Choque and Almendras, 2012). Available stratigraphic, paleocurrent, and structural data are integrated into five paleogeographic map-view reconstructions (Fig. 8) and schematic reconstructions depicting east-west cross-sectional profiles (Fig. 9). Although shown at a regional scale, the proposed sedimentary and tectonic configurations are most directly applicable to the southern Bolivia (R1) study region at 21–23°S.

7.1. Neoproterozoic–Cambrian: eastern cratonic sources to a clastic continental shelf

Upper Neoproterozoic–Cambrian deposits recorded westward sediment transport to a newly established continental shelf that succeeded precursor extensional basins (Fig. 8A). Detrital zircon populations (Figs. 5 and 7) show a combination of: (1) distributed Paleoproterozoic to mid-Neoproterozoic ages indicative of distal eastern sediment sources such as the Amazonian craton (chiefly the Sunsás belt) and Río de la Plata craton; and (2) late Neoproterozoic-Cambrian ages from more local sources in the Brasiliano and Pampean belts, including the Pampean magmatic arc (Fig. 8A) (e.g., Jèzek et al., 1985; Aceñolaza and Toselli, 2009; Ramos et al., 2010; Adams et al., 2011; Escayola et al., 2011; Toselli et al., 2012; Rapela et al., 2016; Casquet et al., 2018). The local sources were most prevalent in northern Argentina and southern Bolivia (R1 and R2), where a clastic continental shelf succeeded the extensional Puncoviscana basin. Farther north (R4), distal cratonic sources fed a segment of the continental shelf that developed after abandonment of the Tucavaca aulacogen (Litherland et al., 1989; Babinski et al., 2013).

Shallow-marine deposition was followed by final Brasiliano-Pampean magmatism, deformation, and low-grade metamorphism of Puncoviscanan-Tucavaca basin fill, which created a regional unconformity within the Cambrian succession (Fig. 3). Across the central Andes, the thick Paleozoic succession deposited above this unconformity (R1-R5; Fig. 2) shows markedly different depositional systems, sediment routing patterns, and provenance signatures (Fig. 7).

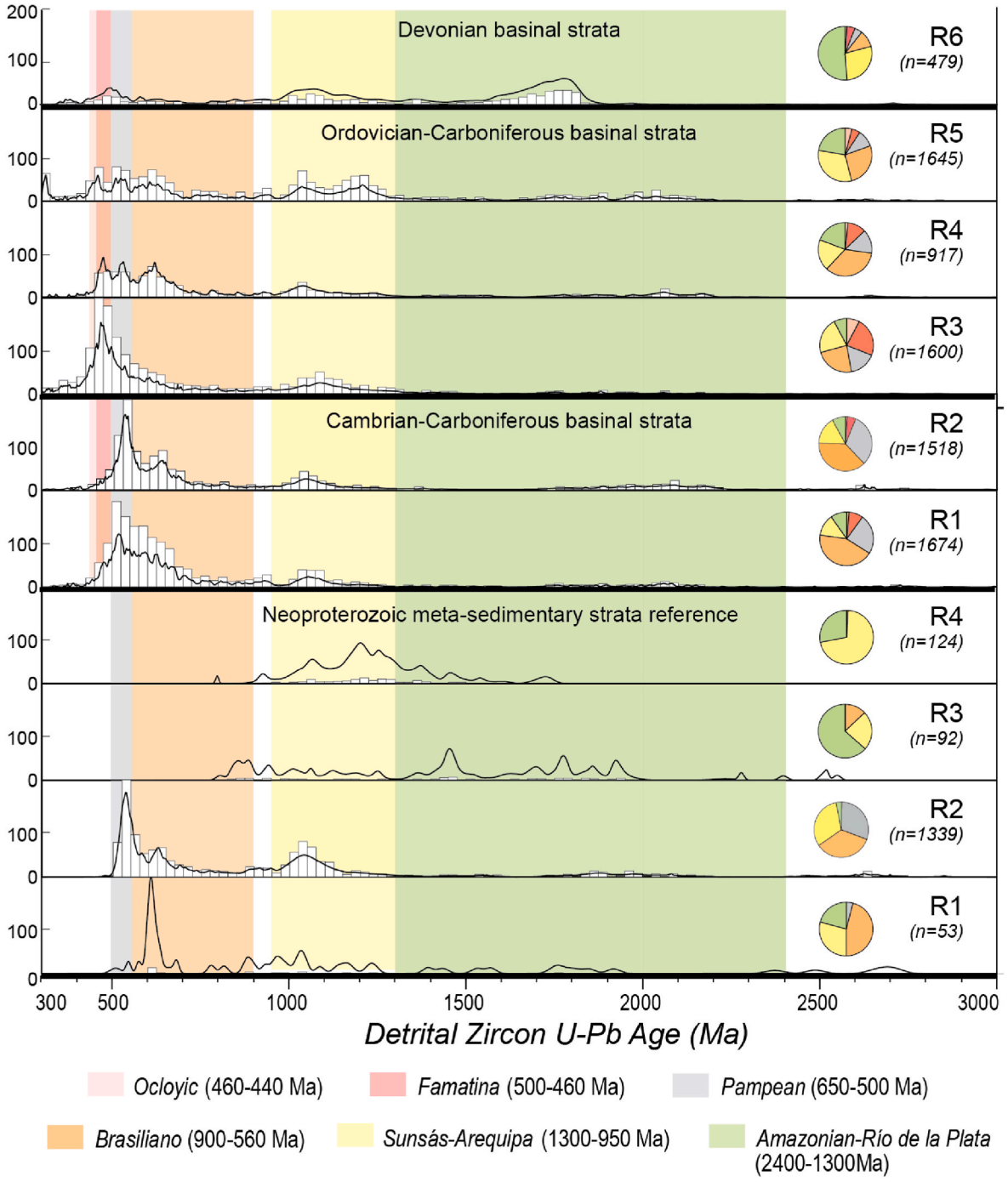

Fig. 7. Composite probability density functions, age histograms and pie diagrams for Neoproterozoic and Paleozoic rocks in the central Andes (regions R1 to R6) generated using detritalPy algorithm (Sharman et al., 2018). The age distributions are normalized, with color shading highlighting distinct age groups representative of different sediment source regions. Horizontal black lines separate samples from different rock successions. Fig. 8F depicts the geographic area of the U–Pb data regions; R1, this study. Table S2 available in the Supplementary data lists the references for detrital zircon studies synthesized in this figure.

7.2. Ordovician: magmatic arc and cratonic sources to a deep marine back-arc basin

Deposition of the >12 km-thick Ordovician clastic succession involved sediment input from the opposing western and eastern flanks of a deep-marine back-arc basin (Fig. 8B). Continued derivation from eastern sources is registered by Neoproterozoic–Cambrian age groups indicative of Pampean and Brasiliano sources, with potential local recycling of metasedimentary Puncoviscana basin fill (Fig. 5C–F). In contrast, the sharp introduction of syndepositional Ordovician zircons attests to input from the newly developed Famatinian magmatic arc in offshore regions to the west (Fig. 5D–F and S1). In southern Bolivia and northern Argentina (R1 and R2), the shale-rich Ordovician succession (Fig. 3) was dominated by deep-marine turbiditic systems with deltaic and shallow-marine systems restricted to eastern localities (e.g., Egenhoff and Lucassen, 2003; Egenhoff, 2007; Moya, 2015).

Sediment delivery from the eastern and western flanks was complemented by longitudinal transport along the N-trending axis of the Famatinian backarc basin (Fig. 8B). Farther north, in northern Bolivia and southern Peru (R4 and R5), Ordovician deposits recorded greater

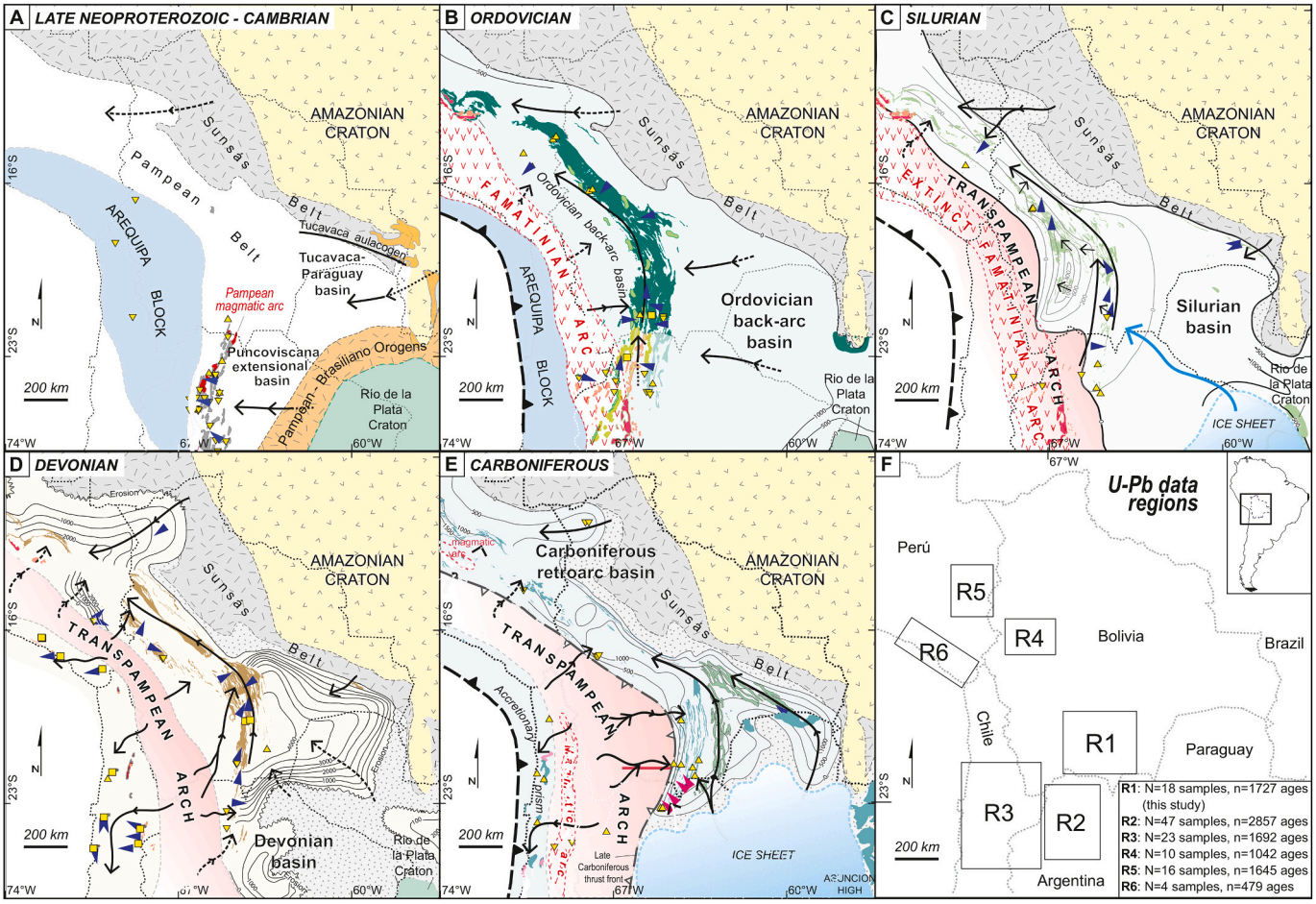

Fig. 8. Schematic paleogeographic reconstructions showing the Neoproterozoic to Carboniferous configuration of tectonic provinces, accreted terranes, and active sedimentary basins in west-central South America. Each panel (A–E) shows the map-view distribution of metamorphic and igneous activity with respect to subduction zones. The inferred basin configuration is represented by the present-day exposures of stratigraphic units (shaded color polygons), stratigraphic thicknesses (isopach data), and sediment transport pathways (arrows). Also shown are the positions of glacial systems.
(A) Neoproterozoic-Cambrian: eastern sediment sources (Brasiliano belt, Amazon craton, and Pampean magmatic arc) fed the Puncoviscana and Tucavaca-Paraguay basins. Sources of data for basement and basinal configuration: Gohrbandt (1992); Loewy et al. (2004); McLeod et al. (2013); Cordani et al. (2010b); Ramos et al. (2010); Basei et al. (2010). Paleocurrent data primary sources: Jêzek et al., 1985; Aceñolaza and Toselli (2009). (B) Ordovician: a >10 km thick back-arc basin was fed by clastic sediment from the Famatinian magmatic arc in the west and Brasiliano and Amazon cratonic sources in the east, during regional extension, trench rollback, and re-accretion of Arequipa-Antofalla to western South America. Sources of data for basinal configuration and magmatism distribution: Gohrbandt, 1992; Avila-Salinas (1992); Sempere (1995); Suárez-Soruco (2000); Choque and Almendras (2012); Loewy et al. (2004); Egenhoff (2007); Coira et al. (2009); Pankhurst et al. (2016); Miskovic et al. (2009); Reimann et al. (2010); Chew et al. (2016). Paleocurrent data primary sources: Egenhoff (2007); Reimann et al. (2010). Thickness data source: Wiens, 1995. (C) Silurian: a southeastern source (Río de la Plata) marked sediment delivery during the Early Silurian glaciation. Eastward growth of the orogen and erosion of relict Famatinian magmatic arc with minor contributions from the Amazonian craton supplemented sediments to initial deep marine basin, which were distributed axially north and northwestward. Primary sources of stratigraphic data: Sempere (1995); Arispe and Díaz-Martinez (1996); Coira et al. (2009); Díaz-Martínez and Grahn (2007); Schönian and Egenhoff (2007). Paleocurrent data primary sources: Sempere (1995); Limachi et al. (1996); Schönian and Egenhoff (2007); Reimann et al. (2010). Thickness data sources: Gohrbandt, 1992; Reutter et al. (1994); Wiens (1995). (D) Devonian: a >4 km thick westward-thickening foreland basin received sediments from a dominantly western source, the Famatinian magmatic arc was extinct by this time, but the broad orogenic growth of the Transpampean Arch shed sediments axially to the north and northeast, as fingerprinted by Famatinian, Ocloyic, and cosmopolitan Pampean, Brasiliano, and Sunsás-Arequipa ages. Primary sources of outcrop and subcrop data: Gohrbandt, 1992; Sempere (1995); Arispe and Díaz-Martinez (1996); Bahlburg and Hervé (1997); Coira et al. (2009); Dalenz et al. (2016); Pankhurst et al. (2016). Paleocurrent data primary sources: Bell (1982); Limachi et al. (1996); Reimann et al. (2010). Thickness data sources: Isaacson and Sablock, 1988; Gohrbandt, 1992; Wiens (1995). (E) Carboniferous: sediment sources in the south and east fed a >1 km thick successor to foreland basin with substantial Neoproterozoic Pampean and Puncoviscana ages during the late Paleozoic age. Glacially influenced marine and nonmarine deposits record NNW-trending longitudinal transport from southern Gondwanan ice sheets. Minor Famatinian and Carboniferous syndepositional zircon ages support renewed subduction and eastward pre-Andean orogenic growth. Primary sources of data: Tankard et al. (1995); Bahlburg and Hervé, 1997; Starck and del Papa (2006); Miskovic et al. (2009); Bache et al. (2012); Chew et al. (2016); Pankhurst et al. (2016). Thickness data sources: Gohrbandt, 1992; Reutter et al. (1994); Wiens (1995). (F) Location of six studied regions (R1-R6) with published U–Pb detrital zircon results that help constrain sediment dispersal patterns. (G) Explanation of patterns and symbols used in the paleogeographic maps.

input from Mesoproterozoic–Cambrian sources to the east, including the Amazonian craton (Fig. 7; Reimann et al., 2010).

7.3. Silurian–Devonian: relict magmatic arc, orogenic, and cratonic sources to foreland basin

The Silurian-Devonian succession reflects erosion of a relict

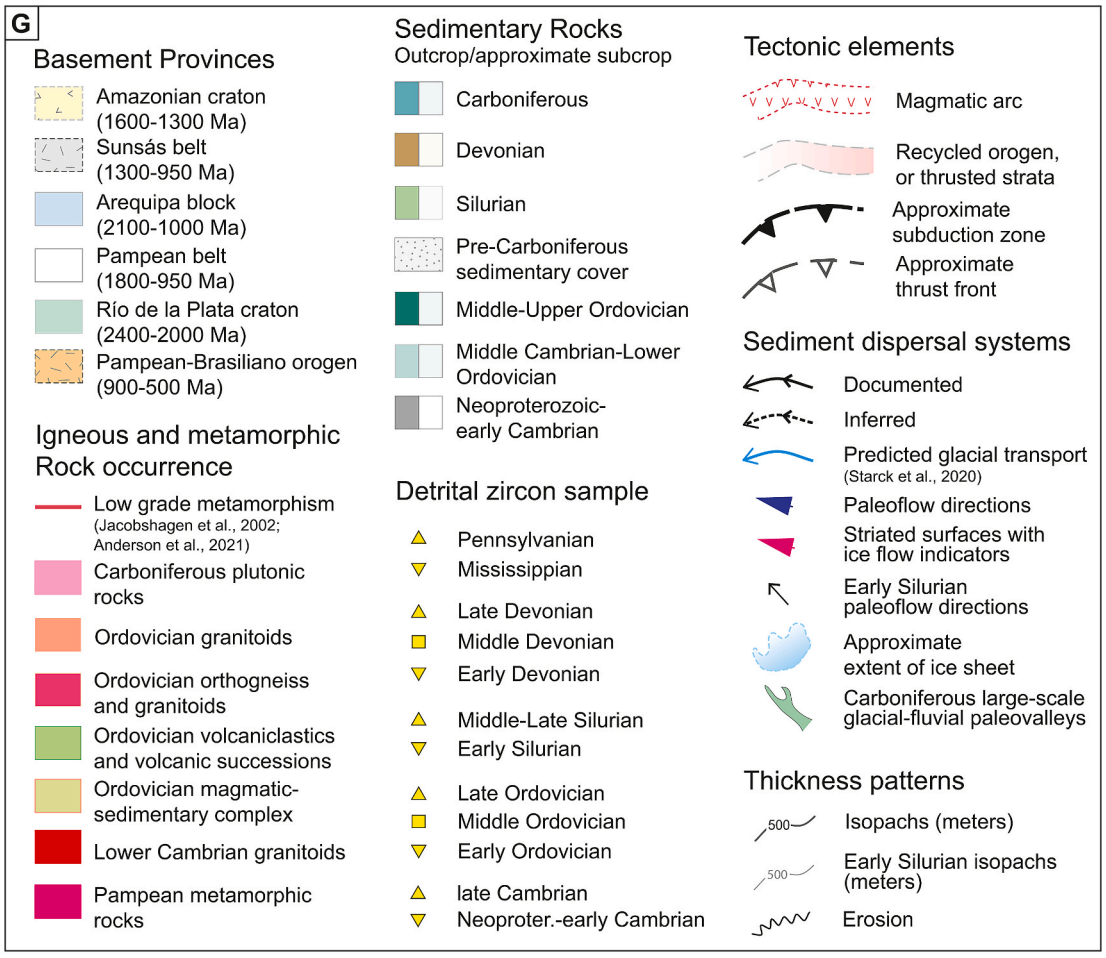

Fig. 8. (*continued*).

magmatic arc and emerging pre-Andean highlands in the west, along with distal cratonic sources to the southeast (Fig. 8C–D). The diverse provenance is shown by cosmopolitan U–Pb age distributions (Fig. 5G–K) that include major Ordovician (Famatinian-Ocloyic) and late Neoproterozoic–Cambrian (Pampean) age signatures with broadly distributed Neoproterozoic (Brasiliano) and Mesoproterozoic (Sunsás-Arequipa) ages. Growth of a contractional orogenic belt to the west (Transpampean Arch), potentially during the Chañic phase of deformation, was responsible for exhumation of the relict Famatinian arc, Ocloyic metamorphic belt, and Arequipa basement (Fig. 8). These western sources distributed sediment eastward and axially northward to fluvial, deltaic, narrow continental shelf, and deep submarine canyons and fan environments within an adjacent, westward-thickening Silurian-Devonian foreland basin (Pádula et al., 1967; Isaacson, 1975; Gohrbandt, 1992; Díaz-Martínez and Grahn, 2007; Augustsson et al., 2015).

A continued, albeit diminished, role of eastern sources is evidenced in Precambrian ages that can be attributed to the Amazonian craton (Sunsás and Río Apa belts), with minimal influence of the Rio de la Plata craton (Fig. 8C). Finally, although syndepositional detrital zircons are rare, minor pre-Andean magmatism of Devonian age is indicated by U–Pb zircon ages from this study (Fig. 5 and S1) and igneous pebbles, diamictite matrix, and sandstones of Carboniferous successions of western Bolivia (Arntzen et al., 2018; López et al., 2018).

7.4. Carboniferous: orogenic and cratonic sources during regional glaciation

Carboniferous accumulation of glacially influenced marine and nonmarine deposits was influenced by pre-Andean highlands and regionally extensive ice sheets of southern Gondwana (Fig. 8E). An abrupt increase in Neoproterozoic detritus is consistent with contributions from Pampean and Puncoviscana sources to the south and east (Fig. 5L–Q). Erosion of these source regions is evidenced by longitudinal transport in NNW-trending glacially carved valleys with >500 m-relief (Tankard et al., 1995; Starck, 1995; Starck and del Papa, 2006; di Pasquo, 2007; Bache et al., 2012). Distal derivation of age-equivalent deposits farther to the south and east (in Argentina and Brazil) highlights the long-distance transport of sediment from southern Gondwanan ice sheets during the late Paleozoic ice age (e.g., Griffis et al., 2018; Craddock et al., 2019; Starck et al., 2021).

In contrast to Devonian deposits, detrital provenance results for clastic fill within the Carboniferous successor to foreland basin show diminished input from a western magmatic arc (Figs. 5 and 6). However, the continued influence of the broad Transpampean Arch is recorded by westward thinning and pinchout of Carboniferous strata to the west (Fig. 2). Westward onlap onto this post-deformational (post-Chañic) basement high during neutral tectonic conditions was followed by renewed shortening and eastward deformation advance during Gondwanide orogenesis (Anderson et al., 2021). Moreover, the presence of syndepositional zircons of Carboniferous age (Fig. 5 and S1) supports the suggestion that isolated alpine glaciers nucleated on pre-Andean highlands may have provided local input from western orogenic sources (Fig. 8E) (e.g., Díaz-Martínez, 1996; Isbell et al., 2012).

8. Discussion

Insights from detrital geochronological results (Figs. 4–6) combined with past provenance datasets (Fig. 7) and paleogeographic constraints

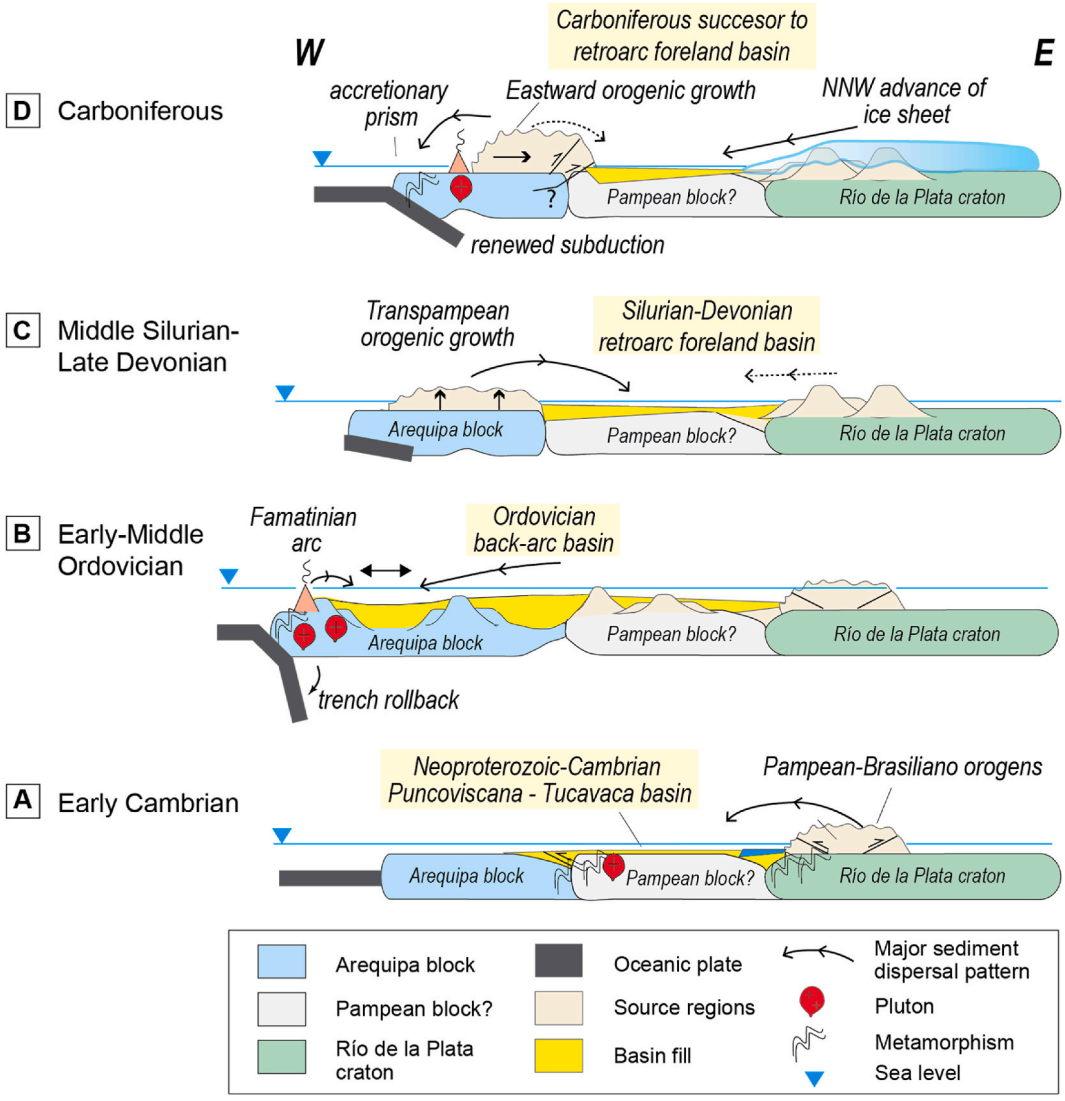

Fig. 9. Schematic east-west cross sections showing Neoproterozoic-Carboniferous tectonic reconstructions, major sediment dispersal systems and basin configurations for southern Bolivia-northern Argentina (~22–23°S).

(Fig. 8) highlight key stages in the pre-Andean history of sediment dispersal and basin evolution along the western Gondwanan margin. These stages are represented in schematic Neoproterozoic–Carboniferous cross-section reconstructions that identify the major tectonic events that have dictated the spatial and temporal distribution of sediment sources (Fig. 9). This synthesis, which focuses on the southern Bolivia to northern Argentina (~22–23°S) segment of the central Andes, not only confirms the overall accretionary character of the plate margin, but also indicates a complex pattern of contrasting pre-Andean tectonic regimes. The following discussion addresses the broader implications for evolution of the western margin of Gondwana, including drivers for subsidence patterns across west-central South America.

8.1. Neoproterozoic–Cambrian: post-extensional Brasiliano-Pampean orogenesis and metamorphism

The Neoproterozoic–Cambrian record involved multiple tectonic events that shaped the sedimentary and structural configuration of the central Andes. Deposition of a >3 km-thick marine succession (Figs. 2 and 3) initiated in the late Neoproterozoic within the Puncoviscana-Tucavaca basin, a regional extensional basin or passive continental margin (Fig. 9A) (Ramos et al., 2010), which received sediment from eastern cratonic sources (Amazonian and Rio de la Plata cratons), basement sources (Brasiliano and Pampean blocks), and coeval magmatic sources (Pampean magmatic arc) (Fig. 5A and B, 7, and 8A).

Closure of this basin during final Brasiliano-Pampean orogenesis and low-grade metamorphism generated a regional angular unconformity within the Cambrian record (Figs. 2 and 3) that provides a critical baseline for the ensuing Paleozoic evolution of central Andean regions (Fig. 9B) (Basei et al., 2010; Ramos, 1988, 2008; Rapela et al., 1998; Lucassen et al., 2000; Suárez-Soruco, 2000; Ramos et al., 2010; Escayola et al., 2011). Following mid to late Cambrian extensional collapse of the Pampean orogen, subduction, arc magmatism, and regional subsidence commenced along this segment of the western Gondwanan margin (Fig. 9C) (Sanchez and Salfity, 1999; Aceñolaza, 2003; Augustsson et al., 2011).

8.2. Ordovician: back-arc extension, Famatinian arc magmatism, and Ocloyic orogenesis

The >12 km-thick Ordovician succession (Figs. 2 and 3) chronicled accumulation in a deep-marine back-arc basin associated with extension in the overriding plate of a retreating subduction system (Fig. 9D)

(Egenhoff, 2007). Deep-sea fans and flanking deltaic systems were fed mud-rich sediments by opposing eastern sources (exhumed Brasiliano-Pampean basement and recycled Puncoviscana basin fill) and a western magmatic arc (Fig. 5C–F and 8B). The Famatinian magmatic arc was established in an offshore position above an east-dipping subduction zone that spanned much of western Gondwana (e.g., Miskovic et al., 2009; Horton et al., 2010; Romero et al., 2013; Chew et al., 2016).

Fault-controlled and thermal subsidence accompanied tholeiitic magmatism, calc-alkaline magmatism, and volcanogenic massive sulfide mineralization generated by back-arc extension during trench rollback and westward arc retreat (e.g., Coira et al., 1982, 2009; Tistl, 1985; Rapela et al., 1998; Arce-Burgoa, 2007; Egenhoff, 2007; Niemeyer et al., 2018). The termination of back-arc extension and extinction of Famatinian arc magmatism is marked by the Ocloyic orogeny, with a corresponding angular unconformity in the Upper Ordovician–Lower Silurian section of Bolivia and northern Argentina (Figs. 2 and 3). Ocloyic deformation involved shortening and eastward translation of the fringing Famatinian magmatic arc and underlying continental basement of the Arequipa terrane (Coira et al., 1982, 2009; Mon and Salfity, 1995; Bahlburg and Hervé, 1997; Moya, 2015). In central Peru, similar closure of a narrow ocean basin induced collision of the continental Paracas terrane against South America with attendant metamorphism (Willner et al., 2014; Ramos, 2018).

8.3. Silurian–Devonian: initiation of pre-Andean foreland basin

Silurian–Devonian tectonic reorganization in central Andean regions involved a shift to a contractional or transpressional setting associated with initial development of an asymmetric foreland basin (Fig. 9E) (Sempere, 1995; Schönian and Egenhoff, 2007). In Bolivia, a >4 km thick, westward-thickening foreland succession of mostly nonmarine and shallow marine strata (Figs. 2 and 3) received sediment from new orogenic sources and relict magmatic-arc sources in the west (principally Arequipa basement and Ordovician Famatinian arc rocks), and subordinate Precambrian sources (Brasiliano-Pampean and Puncoviscana rocks) in the south/southeast (Fig. 5G–K and 8C–D).

Although the absence of widespread arc magmatism suggests the cessation of large-scale subduction, uplift of the Transpampean Arch (largely coincident with the present Altiplano-Puna plateau) during the Chañic orogenic phase is evidenced through regional stratigraphic and sediment dispersal patterns (Pádula et al., 1967; Tankard et al., 1995; Blanquat et al., 1998; Ramos, 2010b; McGroder et al., 2015; Hervé et al., 2018). The evolution from a narrow Silurian foredeep (Fig. 8C) to a broad Devonian basin (Fig. 8D) suggests the eastward advance of flexural subsidence during the progressive shortening and crustal loading within the Transpampean contractional orogen (Gohrbandt, 1992; Limachi et al., 1996; Schönian and Egenhoff, 2007; Díaz-Martínez and Grahn, 2007; Dalenz et al., 2016).

8.4. Carboniferous: retroarc successor to foreland basin during regional glaciation

The >2 km-thick Carboniferous section recorded glaciomarine and nonmarine deposition in a successor to foreland basin during renewed subduction, arc magmatism, and orogenic exhumation (Fig. 9D) (Tankard et al., 1995; Starck and del Papa, 2006; Pankhurst et al., 2016). Detrital signatures indicate principally pre-Andean (Brasiliano-Pampean and Puncoviscana) and cratonic sources to the south and east, along with the appearance of a new syndepositional magmatic arc to the west (Fig. 5L–Q and 8 E). Westward thinning of Carboniferous basin fill attests to the continued role of the Transpampean Arch, a basement high that remained active during the Gondwanide orogeny and was ultimately overlapped during latest Paleozoic-Mesozoic time (Tosdal, 1996; Loewy et al., 2004; Pankhurst et al., 2016). Deformation in southern Bolivia involving east- and west-vergent thrust faulting and low-grade metamorphism concentrated at ~320–290 Ma (Müller et al., 2002; Jacobshagen et al., 2002; Anderson et al., 2021).

Regional glaciation during the late Paleozoic ice age is considered to have been the principal control on Carboniferous sediment delivery to the region, with large N to NNW-directed transport from southern Gondwana (Fig. 8E). The renewal of arc magmatism in central Andean regions is consistent with proposals of a late Paleozoic initiation of the east-dipping subduction geometry (Oliveros et al., 2020, and references therein) that persisted during the Mesozoic and culminated in Cenozoic Andean orogenesis.

9. Conclusions

The integration of detrital zircon U–Pb results with existing stratigraphic and geochronological databases helps shed light on the Neoproterozoic–Carboniferous paleogeography of eroding source regions, sediment dispersal pathways, and basin development along the western Gondwanan margin in the central Andes of west-central South America.

1. Analysis of the >15–20 km thick clastic succession in southern Bolivia provides an understanding of sediment routing and subsidence patterns in relationship to evolving topographic highlands during variable tectonic regimes. Major sediment sources in the east included Proterozoic basement belts (Brasiliano and Pampean orogens) and more-distal Mesoproterozoic to Archean cratonic regions (Amazonian craton and Rio de la Plata craton). The chief sources in the west included various pre-Andean magmatic arcs (notably the Famatinian arc), retroarc fold-thrust belts (linked to Famatinian-Ocloyic, Chañic, or early Gondwanide orogenesis), and western basement terranes (Arequipa block). The geochronological results provide records of the onset and cessation of separate phases of subduction and arc magmatism along the western edge of South America, as well as the accompanying tectonic regimes that varied among extensional, contractional, and neutral conditions.
2. Diverse basin settings included extensional (rift) and passive-margin basins, extensional back-arc basins, retroarc foreland basins, and subsequent successor basins, with phases of marine and nonmarine sedimentation that were variably dominated by tectonic, magmatic, or glacially generated sediment. Contrasting subsidence mechanisms included: (a) processes in extensional basins linked to normal faulting and the thinning and cooling of continental lithosphere; (b) regional isostatic (flexural) subsidence driven by horizontal shortening and crustal thickening; and (c) possible successor basin conditions during post-deformational, neutral tectonic regimes.
3. Neoproterozoic extension generated a continental shelf fed by west-directed clastic transport from eastern cratonic sources (Amazonian and Rio de la Plata cratons), basement sources (Brasiliano and Pampean blocks), and coeval magmatic sources (Pampean magmatic arc) (Figs. 5, 7 and 8). Basin closure during final Brasiliano-Pampean orogenesis involved mid-Cambrian shortening, low-grade metamorphism, and genesis of a regional angular unconformity (Figs. 2 and 3) that provided the foundation for subsequent Paleozoic basin evolution (Fig. 9).
4. Ordovician accumulation of a >12 km thick deep-marine succession occurred in an extensional back-arc basin in a retreating subduction system (Fig. 9). Most sediment was derived from the Famatinian magmatic arc in a western offshore position above the east-dipping subduction zone that spanned much of western Gondwana. Late Ordovician Ocloyic shortening resulted in uplift and exhumation of the extinguished magmatic arc and underlying continental basement of the Arequipa terrane.
5. Silurian–Devonian shortening-induced uplift of a western basement high (the Transpampean Arch) governed the development of an asymmetric foreland basin (>4 km thick) in which relict magmatic arc and orogenic sources fed eastward transverse and northward axial fluvial and shallow marine depositional systems. Although the absence of arc magmatism suggests the cessation of subduction,

eastward deformation advance during this Chañic orogenic phase prompted a shift from a narrow Silurian foredeep to a broad Devonian foreland basin (Fig. 8).

6. Carboniferous sedimentation involved a complex shift from a post-deformational (post-Chañic) successor basin to a renewed foreland basin produced by Gondwanide shortening. Regional glaciation dominated Carboniferous sediment delivery, with chiefly pre-Andean basement (Puncoviscana, Pampean, and Brasiliano) sources and cratonic sources to the south and east eroded by large ice sheets emanating from southern Gondwana (Fig. 8). The appearance of syndepositional zircons recorded the establishment of a magmatic arc and east-dipping subduction zone along the western Gondwanan margin (Figs. 5 and 8), which regulated Mesozoic and Cenozoic phases of basin growth and Andean orogenesis.

CRediT authorship contribution statement

Amanda Z. Calle: Writing – original draft, Investigation, Formal analysis, Conceptualization. **Brian K. Horton:** Writing – review & editing, Supervision, Funding acquisition. **Raúl García:** Investigation. **Ryan B. Anderson:** Validation. **Daniel F. Stockli:** Resources. **Peter P. Flaig:** Writing – review & editing. **Sean P. Long:** Writing – review & editing, Funding acquisition.

Declaration of competing interest

The authors declare that they have no known competing financial interests or personal relationships that could have appeared to influence the work reported in this paper.

Data availability

The data utilized in this research is available in the Supplementary data section.

Acknowledgments

This research was supported by a U.S. National Science Foundation grant (EAR-1250510) awarded to B.K. Horton and S.P. Long, and research support from the Geological Society of America Graduate Student Research Grant, American Association of Petroleum Geologists Grants-in-Aid, Repsol E&P Bolivia, and the Jackson School of Geosciences at the University of Texas at Austin awarded to A.Z. Calle. We thank R. Limachi, V. Ramirez, R. Matos, O. Arispe, A. Ayaviri, N. Jiménez, E. Requena, H. Guerra, and G. Villacorta for critical insights about regional geology. Field and logistical assistance was provided by O. Quenta, C. Andry, G. Uzeda, and A. Buchizo. Guidance in laboratory procedures was provided by E. Pujols, L. Stockli, and M. Prior. This manuscript benefitted from discussions with L. Jackson, T. Capaldi, G. Gutierrez, B. Weber, H. Bahlburg, A. Aleman, and S. Ramirez, and fieldtrip participants in Bolivia during the 11th South American Symposium on Isotope Geology. We thank the Bureau of Economic Geology for providing partial financial support to open access of this article. Constructive comments from anonymous reviewers and editor A. Folguera significantly improved the manuscript.

Appendix A. Supplementary data

Supplementary data to this article can be found online at https://doi.org/10.1016/j.jsames.2023.104286.

References

Aceñolaza, G.F., 2003. The Cambrian system in northwestern Argentina: stratigraphical and palaeontological framework. Geol. Acta 1, 23–39.

Aceñolaza, F.G., Miller, H., Toselli, A.J., 2002. Proterozoic–early Paleozoic evolution in western South America – A discussion. Tectonophysics 354, 121–137. https://doi.org/10.1016/s0040-1951(02)00295-0.

Aceñolaza, F.G., Toselli, A., 2009. The Pampean Orogen: Ediacaran-Lower Cambrian evolutionary history of central and northwest region of Argentina. Dev. Precambrian Geol. 16, 239–254. https://doi.org/10.1016/S0166-2635(09)01618-1.

Adams, C.J., Miller, H., Aceñolaza, F.G., Toselli, a.J., Griffin, W.L., 2011. The Pacific Gondwana margin in the late Neoproterozoic–early Paleozoic: detrital zircon U–Pb ages from metasediments in northwest Argentina reveal their maximum age, provenance and tectonic setting. Gondwana Res. 19, 71–83. https://doi.org/10.1016/j.gr.2010.05.002.

Anderson, H., 2011. Sedimentology and Biostratigraphy of the Carboniferous Tarija-Chaco Basin, Southern Bolivia: Geodynamic and Paleoclimatic Evolution. Ph.D. dissertation, University of Idaho.

Anderson, R.B., Long, S.P., Horton, B.K., Calle, A.Z., Ramirez, V., 2017. Shortening and structural architecture of the Andean foldthrust belt of southern Bolivia (21°S): implications for kinematic development and crustal thickening of the central Andes. Geosphere 13, 538–558. https://doi.org/10.1130/GES01433.1.

Anderson, R.B., Long, S.P., Horton, B.K., Calle, A.Z., Soignard, E., 2021. Late Paleozoic Gondwanide deformation in the Central Andes: Insights from RSCM thermometry and thermal modeling, southern Bolivia. Gondwana Research 94, 222–242. https://doi.org/10.1016/j.gr.2021.03.002.

Aparicio-González, P.A., Pimentel, M.M., Hauser, N., Moya, M.C., 2014. U-Pb LA-ICP-MS geochronology of detrital zircon grains from low-grade metasedimentary rocks (Neoproterozoic–Cambrian) of the Mojotoro Range, northwest Argentina. J. South Am. Earth Sci. 49, 39–50. https://doi.org/10.1016/j.jsames.2013.10.002.

Arce-Burgoa, O., 2007. Guía a los yacimientos metalíferos de Bolivia: La Paz, Bolivia, SPC Impresores, Minera San Cristóbal and Empresa Minera Unificada S.A. (EMUSA).

Arispe, O., Díaz-Martínez, E., 1996. Consideraciones sobre la estratigrafía y los ambientes sedimentarios del límite Silúrico-Devónico en la región sur y centro del Subandino e Interandino Boliviano. Memorias del XII Congreso Geológico de Bolivia, Tarija, pp. 595–607.

Arntzen, S.K., Olsen, T.M., López, S., di Pasquo, M., Zimmerman, U., Ruud, C., Berndt, J., 2018. Devonian or Carboniferous glaciations in the Bolivian Altiplano: Constraints from detrital zircon age dating. 11th South American Symposium on Isotope Geology, Cochabamba.

Augustsson, C., Rusing, T., Adams, C.J., Chmiel, H., Kocabayoglu, M., Buld, M., Zimmermann, U., Berndt, J., Kooijman, E., 2011. Detrital quartz and zircon combined: the production of mature sand with short transportation paths along the Cambrian west Gondwana margin, northwestern Argentina. J. Sediment. Res. 81, 284–298. https://doi.org/10.2110/jsr.2011.23.

Augustsson, C., Rusing, T., Niemeyer, H., Kooijman, E., Berndt, J., Bahlburg, H., Zimmermann, U., 2015. 0.3 byr of drainage stability along the Palaeozoic palaeo-Pacific Gondwana margin; a detrital zircon study. J. Geol. Soc. London. 172, 186–200. https://doi.org/10.1144/jgs2014-065.

Avila-Salinas, W., 1992. El magmatismo Cámbrico-Ordovícico en Bolivia. In: Gutiérrez-Marco, J.G., Saavedra, J., Rábano, I. (Eds.), Paleozoico Inferior de Iberoamérica. Universidad de Extremadura, pp. 241–253.

Avila-Salinas, W., 1996. Ambiente tectónico del volcanismo Ordovícico en Bolivia. Memorias del XII Congreso Geológico de Bolivia-Tarija, pp. 137–143.

Babinski, M., Boggiani, P.C., Trindade, R.I.F., Fanning, C.M., 2013. Detrital zircon ages and geochronological constraints on the Neoproterozoic Puga diamictites and associated BIFs in the southern Paraguay Belt, Brazil. Gondwana Res. 23, 988–997. https://doi.org/10.1016/j.gr.2012.06.011.

Bache, F., Moreau, J., Rubino, J.L., Gorini, C., Van-Vliet Lanoe, B., 2012. The subsurface record of the late Paleozoic glaciation in the Chaco basin, Bolivia. Geol. Soc. London, Spec. Publ. 257–274. https://doi.org/10.1144/SP368.11.

Bahlburg, H., Hervé, F., 1997. Geodynamic evolution and tectonostratigraphic terranes of northwestern Argentina and northern Chile. Geol. Soc. Am. Bull. 109, 869–884. https://doi.org/10.1130/0016-7606(1997)109<0869:GEATTO>2.3.CO;2.

Basei, M.A.S., Brito Neves, B.B., Siga, O., Babinski, M., Pimentel, M.M., Gaeta Tassinari, C.C., Hollanda, M.H.B., Nutman, A., Cordani, U.G., 2010. Contribution of SHRIMP U-Pb zircon geochronology to unravelling the evolution of Brazilian Neoproterozoic fold belts. Precambrian Res. 183, 112–144. https://doi.org/10.1016/j.precamres.2010.07.015.

Becchio, R., Lucassen, F., Kasemann, S., Franz, G., Viramonte, J., 1999. Geoquímica y sistemática isotópica de rocas metamórficas del Paleozoico inferior. Noroeste de Argentina y Norte de Chile (21 ° -27 ° S). Acta Geol. Hisp. 34, 273–299.

Bell, C., 1982. The lower Paleozoic metasedimentary basement of the coastal ranges of Chile between 25°30' and 27°S. Rev. Geol. Chile 17, 21–29.

Bettencourt, J.S., Leite, W.B., Ruiz, A.S., Matos, R., Payolla, B.L., Tosdal, R.M., 2010. The Rondonian-San Ignacio province in the SW amazonian craton: an overview. J. South Am. Earth Sci. 29, 28–46. https://doi.org/10.1016/j.jsames.2009.08.006.

Bierlein, F.P., Stein, H.J., Coira, B., Reynolds, P., 2006. Timing of gold and crustal evolution of the Palaeozoic south central Andes, NW Argentina-implications for the endowment of orogenic belts. Earth Planet Sci. Lett. 245, 702–721. https://doi.org/10.1016/j.epsl.2006.03.019.

Blanquat, M.D.S., Tikoff, B., Teyssier, C., Vigneresse, J.L., 1998. Transpressional kinematics and magmatic arcs. Geol. Soc. London, Spec. Publ. 135, 327–340. https://doi.org/10.1144/GSL.SP.1998.135.01.21.

Calle, A.Z., Horton, B.K., Limachi, R., Stockli, D.F., Uzeda-Orellana, G.V., Anderson, R.B., Long, S.P., 2018. Cenozoic provenance and depositional record of the Sub-Andean foreland basin during growth of the central Andean fold-thrust belt, southern Bolivia, *in* Zamora Valcarce. In: Zamora Valcarce, G., McClay, K.R., Ramos, V.A. (Eds.), *Petroleum Basins and Hydrocarbon Potential of the Andes of Peru and*, 117. AAPG Memoir, *Bolivia*, pp. 483–530. https://doi.org/10.1306/13622132m1173777.

Campanha, G.A.C., Warren, L., Boggiani, P.C., Grohmann, C.H., Cáceres, A.A., 2010. Structural analysis of the Itapucumí Group in the Vallemí region, northern Paraguay: evidence of a new Brasiliano/Pan-African mobile belt. J. South Am. Earth Sci. 30, 1–11. https://doi.org/10.1016/j.jsames.2010.04.001.

Casquet, C., Fanning, C.M., Galindo, C., Pankhurst, R.J., Rapela, C.W., Torres, P., 2010. The Arequipa massif of Peru: new SHRIMP and isotope constraints on a Paleoproterozoic inlier in the Grenvillian orogen. J. South Am. Earth Sci. 29, 128–142. https://doi.org/10.1016/j.jsames.2009.08.009.

Casquet, C., Dahlquist, J.A., Verdecchia, S.O., Baldo, E.G., Galindo, C., Rapela, C.W., Pankhurst, R.J., Morales, M.M., Murra, J.A., Fanning, C.M., 2018. Review of the Cambrian Pampean orogeny of Argentina; a displaced orogen formerly attached to the Saldania Belt of South Africa. Earth Sci. Rev. 177, 209–225. https://doi.org/10.1016/j.earscirev.2017.11.013.

Castaños, A., Rodrigo, L.A., 1978. Sinopsis estratigráfica de Bolivia–I Parte: Paleozoico. Academia Nacional de Ciencias de Bolivia, p. 146.

Cawood, P.A., 2005. Terra Australis orogen: Rodinia breakup and development of the Pacific and Iapetus margins of Gondwana during the Neoproterozoic and Paleozoic. Earth Sci. Rev. 69, 249–279. https://doi.org/10.1016/j.earscirev.2004.09.001.

Chew, D.M., Schaltegger, U., Kosler, J., Whitehouse, M.J., Gutjahr, M., Spikings, R.A., Miskovic, A., 2007. U-Pb geochronologic evidence for the evolution of the Gondwanan margin of the north-central Andes. Bull. Geol. Soc. Am. 119, 697–711. https://doi.org/10.1130/B26080.1.

Chew, D.M., Pedemonte, G., Corbett, E., 2016. Proto-Andean evolution of the eastern Cordillera of Peru. Gondwana Res. 35, 59–78. https://doi.org/10.1016/j.gr.2016.03.016.

Choque, N., Almendras, O., 2012. Servicio Nacional de Geología y Técnico de Minas. Mapa geológico de Bolivia scale 1:1,000,000, 1 sheet.

Coira, B., Davidson, J., Mpodozis, C., Ramos, V., 1982. Tectonic and magmatic evolution of the Andes of northern Argentina and Chile. Earth Sci. Rev. 18, 303–332. https://doi.org/10.1016/0012-8252(82)90042-3.

Coira, B., Koukharsky, M., Guevara, S.R., Cisterna, C.E., 2009. Puna (Argentina) and northern Chile Ordovician basic magmatism: a contribution to the tectonic setting. J. South Am. Earth Sci. 27, 24–35. https://doi.org/10.1016/j.jsames.2008.10.002.

Cordani, U.G., Brito-Neves, B.B., D'Agrella-Filho, M.S., 2003. From Rodinia to Gondwana: a review of the available evidence from South America. Gondwana Res. 6, 275–283. https://doi.org/10.1016/S1342-937X(05)70402-0.

Cordani, U.G., Fraga, L.M., Reis, N., Tassinari, C.C.G., Brito-Neves, B.B., 2010a. On the origin and tectonic significance of the intra-plate events of Grenvillian-type age in South America: a discussion. J. South Am. Earth Sci. 29, 143–159. https://doi.org/10.1016/j.jsames.2009.07.002.

Cordani, U.G., Teixeira, W., Tassinari, C.C.G., Coutinho, J.M.V., Ruiz, A.S., 2010b. The Río Apa craton in Mato Grosso do sul (Brazil) and northern Paraguay: geochronological evolution, correlations and tectonic implications for Rodinia and Gondwana. Am. J. Sci. 310, 981–1023. https://doi.org/10.2475/09.2010.09.

Cordani, U.G., Teixeira, W., 2007. Proterozoic accretionary belts in the Amazonian craton. Geol. Soc. Am. Spec. Publ. 200, 297–320. https://doi.org/10.1130/2007.1200(14.

Coutts, D.S., Matthews, W.A., Hubbard, S.M., 2019. Assessment of widely used methods to derive depositional ages from detrital zircon populations. Geoscience Frontiers 10, 1421–1435. https://doi.org/10.1016/j.gsf.2018.11.002.

Craddock, J.P., Ojakangas, R.W., Malone, D.H., Konstantinou, A., Mory, A., Bauer, W., Thomas, R.J., Affinati, S.C., Pauls, K., Zimmerman, U., Botha, G., Rochas-Campos, A., Santos, P.R. do, Tohver, E., Riccomini, C., Martin, J., Redfern, J., Horstwood, M., Gehrels, G., 2019. Detrital zircon provenance of Permo-Carboniferous glacial diamictites across Gondwana. Earth Sci. Rev. 192, 285–316. https://doi.org/10.1016/j.earscirev.2019.01.014.

Dalenz, A., Rosales, A., Galvarro, J.S., Hernandez, R.M., Alvarez, L., 2016. Mecanismos complejos de sedimentación durante el Devónico en la zona del Chapare y Boomerang. Dptos. Cochabamba y Santa Cruz-Bolivia. Memorias del XXII Congreso Geológico de Bolivia, 1–5.

DeCelles, P.G., Horton, B.K., 2003. Early to middle Tertiary foreland basin development and the history of Andean shortening in Bolivia. Geol. Soc. Am. Bull. 115, 58–77.

D'el-Rey Silva, L.J.H., Walde, D.H.G., Saldanha, D.O., 2016. The Neoproterozoic-Cambrian Paraguay Belt, central Brazil: Part I– New structural data and a new approach on the regional implications. Tectonophysics 676, 20–41. https://doi.org/10.1016/j.tecto.2016.03.019.

di Pasquo, M., 2007. Update and importance of the Carboniferous and Permian palaeontological records of the Tarija basin. In: Díaz-Martínez, E., Rábano, I. (Eds.), 4th European Meeting on Paleontology and Stratigraphy of Latin America Cuadernos del Museo Geominero, 8. Instituto Geológico y Minero de España, Madrid, pp. 107–112.

Díaz-Martínez, E., 1996. Síntesis estratigráfica y geodinámica del Carbonífero de Bolivia. Memorias del XII Congreso Geológico de Bolivia-Tarija, pp. 355–367.

Díaz-Martínez, E., Grahn, Y., 2007. Early Silurian glaciation along the western margin of Gondwana (Peru, Bolivia and northern Argentina): palaeogeographic and geodynamic setting. Palaeogeogr. Palaeoclimatol. Palaeoecol. 245, 62–81. https://doi.org/10.1016/j.palaeo.2006.02.018.

Dickinson, W.R., Gehrels, G.E., 2009. Use of U-Pb ages of detrital zircons to infer maximum depositional ages of strata: a test against a Colorado Plateau Mesozoic database. Earth Planet Sci. Lett. 288 (1–2), 115–125. https://doi.org/10.1016/j.epsl.2009.09.013.

Ducea, M.N., Otamendi, J.E., Bergantz, G.W., Jianu, D., Petrescu, L., 2015. The origin and petrologic evolution of the Ordovician Famatinian-Puna arc. In: DeCelles, P.G., Ducea, M.N., Carrapa, B., Kapp, P.A. (Eds.), Geodynamics of a Cordilleran Orogenic System: the Central Andes of Argentina and Northern Chile, vol. 212. Geological Society of America Memoir, pp. 125–138. https://doi.org/10.1130/2015.1212(07.

Egenhoff, S.O., 2007. Life and death of a Cambrian–Ordovician basin : an Andean three-act play featuring Gondwana and the Arequipa-Antofalla terrane. In: Linnemann, U., Nance, R.D., Kraft, P., Zulauf, G. (Eds.), The Evolution of the Rheic Ocean: from Avalonian-Cadomian Active Margin to Alleghenian-Variscan Collision, vol. 423. Geological Society of America Special Paper, pp. 511–524. https://doi.org/10.1130/2007.2423(26.

Egenhoff, A.S.O., Lucassen, F., 2003. Chemical and isotopic composition of lower to upper Ordovician sedimentary rocks (central Andes/South Bolivia): implications for their source. J. Geol. 111 (4), 487–497.

Einhorn, J.C., Gehrels, G.E., Vernon, A., Decelles, P.G., 2015. U-Pb zircon geochronology of Neoproterozoic – Paleozoic sandstones and Paleozoic plutonic rocks in the Central Andes (21°S – 26°S). In: DeCelles, P.G., Ducea, M.N., Carrapa, B., Kapp, P.A. (Eds.), Geodynamics of a Cordilleran Orogenic System: the Central Andes of Argentina and Northern Chile, vol. 212. Geological Society of America Memoir, pp. 115–124. https://doi.org/10.1130/2015.1212(06.

Erdtmann, B.D., Kley, J., Muller, J., Jacobshagen, V., 1995. Ordovician basin dynamics and new graptolite data from the Tarija region, Eastern Cordillera, South Bolivia. Seventh Int. Symp. Ordovician Syst. (Society Sediment. Geol.), p. 69. –73.

Escayola, M.P., van Staal, C.R., Davis, W.J., 2011. The age and tectonic setting of the Puncoviscana Formation in northwestern Argentina: an accretionary complex related to Early Cambrian closure of the Puncoviscana Ocean and accretion of the Arequipa-Antofalla block. J. South Am. Earth Sci. 32, 438–459. https://doi.org/10.1016/j.jsames.2011.04.013.

Faleiros, F.M., Pavan, M., Remédio, M.J., Rodrigues, J.B., Almeida, V.V., Caltabeloti, F. P., Pinto, L.G.R., Oliveira, A.A., Pinto de Azevedo, E.J., Costa, V.S., 2016. Zircon U-Pb ages of rocks from the Río Apa cratonic terrane (Mato Grosso do Sul, Brazil): new insights for its connection with the Amazonian craton in pre-Gondwana times. Gondwana Res. 34, 187–204. https://doi.org/10.1016/j.gr.2015.02.018.

Favetto, A., Rocha, V., Pomposiello, C., García, R., Barcelona, H., 2015. A new limit for the NW Río de la Plata craton border at about 24°S (Argentina) detected by magnetotellurics. Geol. Acta 13, 243–254. https://doi.org/10.1344/GeologicaActa2015.13.3.6.

Franz, G., Lucassen, F., Kramer, W., Trumbull, R.B., Romer, R.L., Wilke, H.G., Viramonte, J.G., Becchio, R., Siebel, W., 2006. Crustal evolution at the central Andean continental margin: a geochemical record of crustal growth, recycling and destruction. In: Oncken, O., Chong, G., Franz, G., Giese, P., Götze, H.J., Ramos, V.A., Strecker, M.R., Wigger, P. (Eds.), The Andes Active Subduction Orogeny, pp. 45–64. https://doi.org/10.1007/978-3-540-48684-8_3.

Gagnier, P.Y., Blieck, a., Emig, C.C., Sempere, T., Vachard, D., Vanguestaine, M., 1996. New paleontological and geological data on the Ordovician and Silurian of Bolivia. J. South Am. Earth Sci. 9, 329–347. https://doi.org/10.1016/S0895-9811(96)00018-1.

Geraldes, M.C., Van Schmus, W.R., Condie, K.C., Bell, S., Teixeira, W., Babinski, M., 2001. Proterozoic geologic evolution of the SW part of the Amazonian craton in Mato Grosso state, Brazil. Precambrian Res. 111, 91–128. https://doi.org/10.1016/S0301-9268(01)00158-9.

Geraldes, M.C., Tavares, A.D., Costa, A., Santos, D., 2015. An overview of the Amazonian craton evolution : insights for paleocontinental reconstruction. Int. J. Geosci. 6, 1060–1076. https://doi.org/10.4236/ijg.2015.69084.

Girelli, T.J., Chemale, F., Lavina, E.L.C., Laux, J.H., Bongiolo, E.M., Lana, C., 2018. Granulite accretion to Río de la Plata Craton, based on zircon U-Pb-Hf isotopes: tectonic implications for Columbia supercontinent reconstruction. Gondwana Res. 56, 105–118. https://doi.org/10.1016/j.gr.2017.12.010.

Gohrbandt, K.H.A., 1992. Paleozoic paleogeographic and depositional developments on the central proto-Pacific margin of Gondwana: their importance to hydrocarbon accumulation. J. S. Am. Earth Sci. 6 (4), 267–287.

Griffis, N.P., Montañez, I.P., Fedorchuk, N., Isbell, J., Mundil, R., Vesely, F., Weinshultz, L., Iannuzzi, R., Gulbranson, E., Taboada, A., Pagani, A., Sanborn, M.E., Huyskens, M., Wimpenny, J., Linol, B., Yin, Q.Z., 2018. Isotopes to ice: constraining provenance of glacial deposits and ice centers in west-central Gondwana. Palaeogeogr. Palaeoclimatol. Palaeoecol. 1–14. https://doi.org/10.1016/j.palaeo.2018.04.020.

Grader, G.W., Isaacson, P.E., Diaz-Martinez, E., Pope, M.C., 2008. Pennsylvanian and Permian sequences in Bolivia: direct responses to Gondwana glaciation. In: Fielding, C.R., Frank, T.D., Isbell, J.L. (Eds.), Resolving the Late Paleozoic Ice Age in Time and Space, vol. 441. Geological Society of America Special Paper, pp. 143–159. https://doi.org/10.1130/2008.2441(10.

Hervé, F., Calderon, M., Quezada, P., Rapela, C., Pankhurst, R., Fanning, M., 2018. Devonian Geotectonic Environments along the Chilean Portion of the Gondwana Continental Margin. XV Congreso Geológico Chileno, Concepción, p. 847.

Horton, B.K., 2018a. Tectonic regimes of the central and southern Andes: responses to variations in plate coupling during subduction. Tectonics 37, 402–429. https://doi.org/10.1002/2017TC004624.

Horton, B.K., 2018b. Sedimentary record of Andean mountain building. Earth Sci. Rev. 178, 279–309. https://doi.org/10.1016/j.earscirev.2017.11.025.

Horton, B.K., Saylor, J.E., Nie, J., Mora, A., Parra, M., Reyes-Harker, A., Stockli, D.F., 2010. Linking sedimentation in the northern Andes to basement configuration, Mesozoic extension, and Cenozoic shortening: evidence from detrital zircon U-Pb ages, Eastern Cordillera, Colombia. Geol. Soc. Am. Bull. 122, 1423–1442. https://doi.org/10.1130/B30118.1.

Horton, B.K., Capaldi, T.N., Perez, N.D., 2022. The role of flat slab subduction, ridge subduction, and tectonic inheritance in Andean deformation. Geology 50, 1007–1012. https://doi.org/10.1130/G50094.1.

Horton, B.K., Fuentes, F., Boll, A., Starck, D., Ramirez, S.G., Stockli, D.F., 2016. Andean stratigraphic record of the transition from backarc extension to orogenic shortening:

a case study from the northern Neuquén basin, Argentina. J. S. Am. Earth Sci. 71, 17–40. https://doi.org/10.1016/j.jsames.2016.06.003.
Hueck, M., Oyhantçabal, P., Philipp, R.P., Basei, M.A.S., Siegesmund, S., 2018. The Dom Feliciano belt in southern Brazil and Uruguay. In: Siegesmund, S., Basei, M.A.S., Oyhantçabal, P., Oriolo, S. (Eds.), The Geology of Southwest Gondwana. Springer International Publishing, pp. 267–302.
Ibanez-Mejia, M., Pullen, A., Arenstein, J., Gehrels, G.E., Valley, J., Ducea, M.N., Mora, A.R., Pecha, M., Ruiz, J., 2015. Unraveling crustal growth and reworking processes in complex zircons from orogenic lower-crust : the Proterozoic Putumayo Orogen of Amazonia. Precambrian Res. 267, 285–310. https://doi.org/10.1016/j.precamres.2015.06.014.
Isaacson, P.E., 1975. Evidence for a western extracontinental land source during the Devonian period in the Central Andes. Bull. Geol. Soc. Am. 86, 39–46. https://doi.org/10.1130/0016-7606(1975)86<39:EFAWEL>2.0.CO;2.
Isaacson, P.E., Sablock, P.E., 1988. Devonian system in Bolivia, Peru, and northern Chile. Canadian Society of Petroleum Geologists Memoir 14, 719–728.
Isaacson, P.E., Díaz-Martínez, E., 1995. Evidence for a middle-late Paleozoic foreland basin and significant paleolatitudinal shift, Central Andes. In: Tankard, A., Suárez, R., Welsink, H.J. (Eds.), Petroleum Basins of South America: American Association of Petroleum Geologists Memoir, vol. 62, pp. 231–250.
Isbell, J.L., Henry, L.C., Gulbranson, E.L., Limarino, C.O., Fraiser, M.L., Koch, Z.J., Ciccioli, P.L., Dineen, A.A., 2012. Glacial paradoxes during the late Paleozoic ice age: evaluating the equilibrium line altitude as a control on glaciation. Gondwana Res. 22, 1–19. https://doi.org/10.1016/j.gr.2011.11.005.
Jackson, S.E., Pearson, N.J., Griffin, W.L., Belousova, E.A., 2004. The application of laser ablation-inductively coupled plasma-mass spectrometry to in situ U – Pb zircon geochronology. Chem. Geol. 211 (1–2), 47–69. https://doi.org/10.1016/j.chemgeo.2004.06.017.
Jacobshagen, V., Müller, J., Wemmer, K., Ahrendt, H., Manutsoglu, E., 2002. Hercynian deformation and metamorphism in the Cordillera Oriental of southern Bolivia, central Andes. Tectonophysics 345, 119–130. https://doi.org/10.1016/S0040-1951(01)00209-8.
Jaillard, E., Heráil, G., Monfret, T., Díaz-Martínez, E., Baby, P., Lavenu, A., Dumont, D.F., 2000. Tectonic evolution of the Andes of Ecuador, Peru, Bolivia and northernmost Chile. In: Cordani, U.G., Milani, E.J., Thomaz Filho, A., Campos, D.A. (Eds.), Tectonic Evolution of South America. 3[1s]t International Geological Congress, Rio de Janeiro, pp. 635–685.
Jêzek, P., Willner, A.P., Aceñolaza, F.G., Miller, H., 1985. The Puncoviscana trough–- a large basin of Late Precambrian to Early Cambrian age on the Pacific edge of the Brazilian shield. Geol. Rundsch. 74, 573–584. https://doi.org/10.1007/BF01821213.
Jiménez, N., 2018. Precambrian Basement Ages of the Altiplano as Inferred from Reworked Zircons in Cenozoic Volcanic Rocks, Western Bolivia, vol. 85. 11th South American Symposium on Isotope Geology, Cochabamba.
Kley, J., 1996. Transition from basement-involved to thin-skinned thrusting in the Cordillera Oriental of southern Bolivia. Tectonics 15 (4), 763–775. https://doi.org/10.1029/95TC03868.
Kley, J., Müller, J., Tawackoli, S., Jacobshagen, V., Manutsoglu, E., 1997. Preandean and Andean-age deformation in the Eastern Cordillera of southern Bolivia. J. S. Am. Earth Sci. 10, 1–19. https://doi.org/10.1016/S0895-9811(97)00001-1.
Kley, J., Monaldi, C.R., Salfity, J.A., 1999. Along-strike segmentation of the Andean foreland: causes and consequences. Tectonophysics 301, 75–94. https://doi.org/10.1016/S0040-1951(98)90223-2.
Lehmann, B., 1978. A Precambrian core sample from the Altiplano/Bolivia. Geol. Rundsch. 67 (1), 270–278.
Levina, M., Horton, B.K., Fuentes, F., Stockli, D.F., 2014. Cenozoic sedimentation and exhumation of the foreland basin system preserved in the Precordillera thrust belt (31–32°S), southern central Andes, Argentina. Tectonics 33, 1659–1680. https://doi.org/10.1002/2013TC003424.
Limachi, R., Goitia, V.H., Sarmiento, D., Arispe, O., Montecinos, R., Martinez, E.D., Farjat, A.O., Liachenco, N., Leyton, M.P., Aguilera, E., 1996. Estratigrafía, geoquímica, correlaciones, ambientes sedimentarios y bioestratigrafía del Silúrico-Devónico de Bolivia. Memorias del XII Congreso Geológico de Bolivia, pp. 183–197.
Litherland, M., Annells, R.N., Darbyshire, D.P.F., Fletcher, C.J.N., Hawkins, M.P., Klinck, B.A., Mitchell, W.I., O'Connor, E.A., Pitfield, P.E.J., Power, G., Webb, B.C., 1989. The Proterozoic of Eastern Bolivia and its relationship to the Andean mobile belt. Precambrian Res. 43, 157–174. https://doi.org/10.1016/0301-9268(89)90054-5.
Litherland, M., Bloomfield, K., 1981. The Proterozoic history of eastern Bolivia. Precambrian Res. 15, 157–179.
Loewy, S.L., Connelly, J.N., Dalziel, I.W.D., 2004. An orphaned basement block: the Arequipa-Antofalla Basement of the central Andean margin of South America. Geol. Soc. Am. Bull. 116, 171. https://doi.org/10.1130/B25226.1.
López, S., Gareca, M.R., Mendoza, G.C., Zimmermann, U., Ruud, C., Berndt, J., 2018. Provenance of the Carboniferous to Permian Copacabana Formation of the Bolivian Altiplano, vol. 91. 11th South American Symposium on Isotope Geology, Cochabamba.
Lucassen, F., Becchio, R., Wilke, H.G., Franz, G., Thirlwall, M.F., Viramonte, J., Wemmer, K., 2000. Proterozoic–- Paleozoic development of the basement of the Central Andes (18 – 26°S) – a mobile belt of the South American craton. J. South Am. Earth Sci. 13, 697–715.
McGroder, M.F., Lease, R.O., Pearson, D.M., 2015. Along-strike variation in structural styles and hydrocarbon occurrences, Subandean fold-and-thrust belt and inner foreland, Colombia to Argentina. In: DeCelles, P.G., Ducea, M.N., Carrapa, B., Kapp, P.A. (Eds.), Geodynamics of a Cordilleran Orogenic System: the Central Andes of Argentina and Northern Chile, vol. 212. Geological Society of America Memoir, pp. 79–113. https://doi.org/10.1130/2015.1212(05.
McLeod, C.L., Davidson, J.P., Nowell, G.M., de Silva, S.L., Schmitt, A.K., 2013. Characterizing the continental basement of the central Andes: constraints from Bolivian crustal xenoliths. Bull. Geol. Soc. Am. 125, 985–997. https://doi.org/10.1130/B30721.1.
McQuarrie, N., Horton, B., Zandt, G., Beck, S., Decelles, P., 2005. Lithospheric evolution of the Andean fold-thrust belt, Bolivia, and the origin of the central Andean plateau. Tectonophysics 399, 15–37. https://doi.org/10.1016/j.tecto.2004.12.013.
Miranda, A.P., Souza, C.E., Melo, J.H.G., Oller, J., 2003. Sequence stratigraphy of the late Silurian–Devonian Subandean basin in southern Bolivia & northern Argentina. VIII simp. Boliv.–- Explor. Pet. en las Cuencas Subandinas 297–308.
Miskovic, A., Spikings, R.A., Chew, D.M., Kosler, J., Ulianov, A., Schaltegger, U., 2009. Tectonomagmatic evolution of Western Amazonia: geochemical characterization and zircon U-Pb geochronologic constraints from the Peruvian Eastern Cordilleran granitoids. Geol. Soc. Am. Bull. 121, 1298–1324. https://doi.org/10.1130/B26488.1.
Mon, R., Salfity, A., 1995. Tectonic evolution of the Andes of northern Argentina. In: Tankard, A., Suárez, R., Welsink, H.J. (Eds.), Petroleum Basins of South America: American Association of Petroleum Geologists Memoir, vol. 62, pp. 269–284.
Moya, M.C., 2015. La "Fase Oclóyica" (Ordovícico Superior) en el noroeste Argentino. Interpretación histórica y evidencias en contrario. Ser. Correlación Geol. 31, 73–110.
Müller, J.P., Kley, J., Jacobshagen, V., 2002. Structure and Cenozoic kinematics of the Eastern Cordillera, southern Bolivia (21°S). Tectonics 21, 1–23. https://doi.org/10.1029/2001TC001340.
Niemeyer, H., Götze, J., Sanhueza, M., Portilla, C., 2018. The Ordovician magmatic arc in the northern Chile-Argentina Andes between 21° and 26° south latitude. J. South Am. Earth Sci. 81, 204–214. https://doi.org/10.1016/j.jsames.2017.11.016.
Oliveros, V., Vásquez, P., Creixell, C., Lucassen, F., Ducea, M.N., Ciocca, I., González, J., Salazar, E., Coloma, F., Kasemann, S.A., 2020. Lithospheric evolution of the pre-and early Andean convergent margin, Chile. Gondwana Res. 80, 202–227.
Omarini, R.H., Sureda, R.J., Götze, H.J., Seilacher, A., Pflüger, F., 1999. Puncoviscana folded belt in northwestern Argentina: testimony of Late Proterozoic Rodinia fragmentation and pre-Gondwana collisional episodes. Int. J. Earth Sci. 88, 76–97. https://doi.org/10.1007/s005310050247.
Oriolo, S., Oyhant abal, P., Wemmer, K., Heidelbach, F., Pf nder, J., Basei, M.A.S., Hueck, M., Hannich, F., Sperner, B., Siegesmund, S., 2016. Shear zone evolution and timing of deformation in the Neoproterozoic transpressional Dom Feliciano belt, Uruguay. J. Struct. Geol. 92, 59–78.
Otamendi, J.E., Ducea, M.N., Cristofolini, E.A., Tibaldi, A.M., Camilletti, G.C., Bergantz, G.W., 2017. U-Pb ages and Hf isotope compositions of zircons in plutonic rocks from the central Famatinian arc, Argentina. J. South Am. Earth Sci. 76, 412–426. https://doi.org/10.1016/j.jsames.2017.04.005.
Otamendi, J.E., Cristofolini, E.A., Morosini, A., Armas, P., Tibaldi, A.M., Camilletti, G.C., 2020. The geodynamic history of the Famatinian arc, Argentina: a record of exposed geology over the type section (latitudes 27°- 33° south). J. S. Am. Earth Sci. 100, 102558 https://doi.org/10.1016/j.jsames.2020.102558.
Pádula, E., Rolleri, E., Mingramm, A., Roque Criado, P., Flores, M.A., Baldis, B., 1967. Devonian of Argentina. Actas del Symp. Devonian Syst 165–199.
Pankhurst, R.J., Hervé, F., Fanning, C.M., Calderón, M., Niemeyer, H., Griem-Klee, S., Soto, F., 2016. The pre-Mesozoic rocks of northern Chile: U-Pb ages, and Hf and O isotopes. Earth Sci. Rev. 152, 88–105. https://doi.org/10.1016/j.earscirev.2015.11.009.
Paton, C., Woodhead, J.D., Hellstrom, J.C., Hergt, J.M., Greig, A., Maas, R., 2010. Improved laser ablation U-Pb zircon geochronology through robust downhole fractionation correction. Geochemistry, Geophysics, Geosystems 11 (3). https://doi.org/10.1029/2009GC002618.
Pepper, M., Gehrels, G., Pullen, A., Ibanez-Mejia, M., Ward, K.M., Kapp, P., 2016. Magmatic history and crustal genesis of western South America: constraints from U-Pb ages and Hf isotopes of detrital zircons in modern rivers. Geosphere 12, 1532–1555. https://doi.org/10.1130/GES01315.1.
Petrus, J.A., Kamber, B.S., 2012. VizualAge : a novel approach to laser ablation ICP-MS U-Pb geochronology data reduction. Geostand. Geoanal. Res. 36, 247–270. https://doi.org/10.1111/j.1751-908X.2012.00158.x.
Ramos, V.A., 1988. Late Proterozoic-Early Paleozoic of South America–a collisional history. Episodes 11 (3), 168–174.
Ramos, V.A., 2008. The basement of the central Andes: the Arequipa and related terranes. Annu. Rev. Earth Planet Sci. 36, 289–324. https://doi.org/10.1146/annurev.earth.36.031207.124304.
Ramos, V.A., 2009. Anatomy and global context of the Andes: main geologic features and the Andean orogenic cycle. In: Kay, S.M., Ramos, V.A., Dickinson, W.R. (Eds.), Backbone of the Americas: Shallow Subduction, Plateau Uplift, and Ridge and Terrane Collision. Geological Society of America Memoir 204, pp. 31–65.
Ramos, V.A., 2010a. The Grenville-age basement of the Andes. J. South Am. Earth Sci. 29, 77–91. https://doi.org/10.1016/j.jsames.2009.09.004.
Ramos, V.A., 2010b. The tectonic regime along the Andes : present-day and Mesozoic regimes. Geol. J. 25, 2–25. https://doi.org/10.1002/gj.
Ramos, V.A., Vujovich, G., Martino, R., Otamendi, J., 2010. Pampia: a large cratonic block missing in the Rodinia supercontinent. J. Geodyn. 50, 243–255. https://doi.org/10.1016/j.jog.2010.01.019.
Ramos, V.A., 2018. The Famatinian Orogen along the protomargin of western Gondwana: evidence for a nearly continuous Ordovician magmatic arc between Venezuela and Argentina. In: Folguera, A., et al. (Eds.), The Evolution of the Chilean-Argentinean Andes. Springer Earth System Sciences. Springer, Cham. https://doi.org/10.1007/978-3-319-67774-3_6.

Rapela, C.W., Pankhurst, R.J., Casquet, C., Baldo, E., Saavedra, J., Galindo, C., 1998. Early evolution of the proto-Andean margin of South America. Geology 26, 707–710. https://doi.org/10.1130/0091-7613(1998)026<0707:EEOTPA>2.3.CO.

Rapela, C.W., Pankhurst, R.J., Casquet, C., Fanning, C.M., Baldo, E.G., González-Casado, J.M., Galindo, C., Dahlquist, J., 2007. The Río de la Plata craton and the assembly of SW Gondwana. Earth Sci. Rev. 83, 49–82. https://doi.org/10.1016/j.earscirev.2007.03.004.

Rapela, C.W., Verdecchia, S.O., Casquet, C., Pankhurst, R.J., Baldo, E.G., Galindo, C., Murra, J.A., Dahlquist, J.A., Fanning, C.M., 2016. Identifying Laurentian and SW Gondwana sources in the Neoproterozoic to early Paleozoic metasedimentary rocks of the Sierras Pampeanas: paleogeographic and tectonic implications. Gondwana Res. 32, 193–212. https://doi.org/10.1016/j.gr.2015.02.010.

Rapela, C.W., Pankhurst, R.J., Casquet, C., Dahlquist, J.A., Fanning, C.M., Baldo, E.G., Galindo, C., Alasino, P.H., Ramacciotti, C.D., Verdecchia, S.O., Murra, J.A., Basei, M. A.S., 2018. A review of the Famatinian Ordovician magmatism in southern South America: evidence of lithosphere reworking and continental subduction in the early proto-Andean margin of Gondwana. Earth Sci. Rev. 187, 259–285. https://doi.org/10.1016/j.earscirev.2018.10.006.

Reimann, C.R., Bahlburg, H., Kooijman, E., Berndt, J., Gerdes, A., Carlotto, V., López, S., 2010. Geodynamic evolution of the early Paleozoic Western Gondwana margin 14°–17°S reflected by the detritus of the Devonian and Ordovician basins of southern Peru and northern Bolivia. Gondwana Res. 18, 370–384. https://doi.org/10.1016/j.gr.2010.02.002.

Reutter, K.J., Doebel, R., Bogdanic, T., Kley, J., 1994. Geological map of the central Andes between 20° S and 26°S, scale 1: 1000000. In: Reutter, K.J., Scheuber, E., Wigger, P. (Eds.), Tectonics of the Southern Central Andes, Map Appendix. Springer Verlag, Berlin.

Rocha-Campos, A.C., De Carvalho, R.G., Amos, A.J., 1977. A Carboniferous (Gondwana) fauna from Subandean Bolivia. Revista Brasileira de Geosciencias 7, 287–303.

Romero, D., Valencia, K., Alarcón, P., Peña, D., Ramos, V.A., 2013. The offshore basement of Perú: evidence for different igneous and metamorphic domains in the forearc. J. South Am. Earth Sci. 42, 47–60. https://doi.org/10.1016/j.jsames.2012.11.003.

Sanchez, M.C., Salfity, J.A., 1999. La cuenca Cámbrica del Grupo Mesón en el Noroeste Argentino: desarrollo estratigráfico y paleogeográfico. Acta Geol. Hisp. 34, 123–139.

Santos, J.O.S., Rizzotto, G.J., Potter, P.E., McNaughton, N.J., Matos, R.S., Hartmann, L. A., Chemale, F., Quadros, M.E.S., 2008. Age and autochthonous evolution of the Sunsás orogen in west Amazon craton based on mapping and U–Pb geochronology. Precambrian Res. 165, 120–152. https://doi.org/10.1016/j.precamres.2008.06.009.

Saylor, J.E., Sundell, K.E., 2016. Quantifying comparison of large detrital geochronology data sets. Geosphere 12, 203–220.

Schönian, F., Egenhoff, S.O., 2007. A Late Ordovician ice sheet in South America: evidence from the Cancañiri tillites, southern Bolivia. In: Linnemann, U., Nance, R. D., Kraft, P., Zulauf, G. (Eds.), The Evolution of the Rheic Ocean: from Avalonian-Cadomian Active Margin to Alleghenian-Variscan Collision, vol. 423. Geological Society of America Special Paper, pp. 525–548. https://doi.org/10.1130/2007.2423(27.

Schwartz, J.J., Gromet, L.P., Miró, R., 2008. Timing and duration of the calc-alkaline arc of the Pampean orogeny: implications for the late Neoproterozoic to Cambrian evolution of Western Gondwana. J. Geol. 116 (1), 39–61. https://doi.org/10.1086/524122.

Sempere, T., 1995. Phanerozoic evolution of Bolivia and adjacent regions. In: Tankard, A., Suárez, R., Welsink, H.J. (Eds.), Petroleum Basins of South America: American Association of Petroleum Geologists Memoir, vol. 62, pp. 423–444.

Sharman, G.R., Sharman, J.P., Sylvester, Z., 2018. detritalPy: a Python-based toolset for visualizing and analysing detrital geo-thermochronologic data. The Depositional Record 4 (2), 202–215. https://doi.org/10.1002/dep2.45.

Slama, J., J, K., Condon, D.J., Crowley, J.L., Gerdes, A., Hanchar, J.M., Horstwood, M.S., Morris, G.A., Nasdala, L., Norberg, N., Schaltegger, U., 2008. Plešovice zircon—a new natural reference material for U–Pb and Hf isotopic microanalysis. Chem. Geol. 30 (1–2), 1–35. https://doi.org/10.1016/j.chemgeo.2007.11.005, 249.

Starck, D., 1995. Silurian–Jurassic stratigraphy and basin evolution of northwestern Argentina. In: Tankard, A., Suárez, R., Welsink, H.J. (Eds.), Petroleum Basins of South America: American Association of Petroleum Geologists Memoir, vol. 62, pp. 251–267.

Starck, D., Bordese, S., Guibaldo, C., Hernandez, R., 2021. Size and style of the Gondwana late Paleozoic ice cover: insights from U-Pb dating of the Tarija Formation granitic boulders. J. S. Am. Earth Sci. 106 https://doi.org/10.1016/j.jsames.2020.102954.

Starck, D., del Papa, C., 2006. The northwestern Argentina Tarija Basin: stratigraphy, depositional systems, and controlling factors in a glaciated basin. J. South Am. Earth Sci. 22, 169–184. https://doi.org/10.1016/j.jsames.2006.09.013.

Suárez Soruco, R., 1976. El Sistema Ordovícico de Bolivia. Revista Técnica de YPFB 5 (1), 111–223.

Suárez-Soruco, R., 2000. Compendio de geología de Bolivia. Revista Técnica de YPFB 18, 1–2.

Tankard, A.J., Uliana, M.A., Welsink, H.J., Ramos, V.A., Turic, M., Franca, A.B., Milani, E.J., Brito-Neves, B.B., Eyles, N., Skarmeta, J., Santa Ana, H., Wiens, F., Cirbián, M., López-Paulsen, O., Germs, C.G.B., De Wit, M.J., Machacha, T., Miller, R. M., 1995. Structural and tectonic controls of basin evolution in southwestern Gondwana during the Phanerozoic. In: Tankard, A., Suárez, R., Welsink, H.J. (Eds.), Petroleum Basins of South America: American Association of Petroleum Geologists Memoir, vol. 62, pp. 5–52.

Teixeira, W., Geraldes, M.C., Matos, R., Ruiz, A.S., Saes, G., Vargas-Mattos, G., 2010. A review of the tectonic evolution of the Sunsás belt, SW Amazonian Craton. J. South Am. Earth Sci. 29, 47–60. https://doi.org/10.1016/j.jsames.2009.09.007.

Tistl, M., 1985. Die Goldlagerstätten der nördlichen Cordillera Real/Bolivien und ihr geologischer, vol. 65. Berliner geowiss, Berlin, p. 93. Reimer.

Tosdal, R.M., 1996. The Amazon-Laurentian connection as viewed from the middle Proterozoic rocks in the central Andes, western Bolivia and northern Chile. Tectonics 15, 827–842. https://doi.org/10.1029/95TC03248.

Toselli, A.J., Aceñolaza, G.F., Miller, H., Adams, C., Aceñolaza, F.G., Rossi, J.N., 2012. Basin evolution of the margin of Gondwana at the Neoproterozoic/Cambrian transition: the Puncoviscana Formation of northwest Argentina. Neues Jahrbuch Geol. Palaontol. Abhand. 265, 79–95. https://doi.org/10.1127/0077-7749/2012/0246.

Uba, C.E., Kley, J., Strecker, M.R., Schmitt, A.K., 2009. Unsteady evolution of the Bolivian Subandean thrust belt: the role of enhanced erosion and clastic wedge progradation. Earth Planet Sci. Lett. 281, 134–146. https://doi.org/10.1016/j.epsl.2009.02.010.

Vujovich, G.I., Van Staal, C.R., Davis, W., 2004. Age constraints on the tectonic evolution and provenance of the Pie de Palo complex, Cuyania composite terrane, and the Famatinian orogeny in the sierra de Pie de Palo, San Juan. Gondwana Res. 7, 1041–1056. https://doi.org/10.1016/S1342-937X(05)71083-2. Argentina.

Walde, D.H.G., do Carmo, D.A., Guimarães, E.M., Vieira, L.C., Erdtmann, B.-D., Sanchez, E.A.M., Adorno, R.R., Tobias, T.C., 2015. New aspects of Neoproterozoic-Cambrian transition in the Corumbá region (state of Mato Grosso do Sul, Brazil). Ann. Paleontol. 101, 213–224. https://doi.org/10.1016/j.annpal.2015.07.002.

Wicander, R., Clayton, G., Marshall, J.E.A., Troth, I., Racey, A., 2011. Was the latest Devonian glaciation a multiple event? New palynological evidence from Bolivia. Palaeogeogr. Palaeoclimatol. Palaeoecol. 305, 75–83. https://doi.org/10.1016/j.palaeo.2011.02.016.

Wiens, F., 1995. Phanerozoic tectonics and sedimentation in the Chaco Basin of Paraguay, with comments on hydrocarbon potential. In: Tankard, A., Suárez, R., Welsink, H.J. (Eds.), Petroleum Basins of South America: American Association of Petroleum Geologists Memoir, vol. 62, pp. 185–206.

Willner, A.P., Tassinari, C.C.G., Rodrigues, J.F., Acosta, J., Castroviejo, R., Rivera, M., 2014. Contrasting Ordovician high- and low-pressure metamorphism related to a microcontinent-arc collision in the Eastern Cordillera of Perú (Tarma province). J. South Am. Earth Sci. 54, 71–81. https://doi.org/10.1016/j.jsames.2014.05.001.

Wörner, G., Lezaun, J., Beck, A., Heber, V., Lucassen, F., Zinngrebe, E., Rössling, R., Wilke, H.G., 2000. Precambrian and early Paleozoic evolution of the Andean basement at Belen (northern Chile) and Cerro Uyarani (western Bolivia Altiplano). J. South Am. Earth Sci. 13, 717–737. https://doi.org/10.1016/S0895-9811(00)00056-0.